

# ESTIMATING EVAPOTRANSPIRATION UNDER NONHOMOGENEOUS FIELD CONDITIONS

ARS-NE-51  
April 1975

RETURN TO GOV. DOCS. CLERK

120



Single free copies of this report  
are available on request to:

*U.S. Department of Agriculture*  
Agricultural Research Service  
Northeast Watershed Research Center  
111 Research Building A  
University Park, Pa. 16802

## ACKNOWLEDGMENTS

The authors are indebted to Michael N. Johnson and George M. Drake, technicians, for the fabrication, testing, and operation of the instrumentation used in this study. The authors are also grateful to Dr. E.R. Lemon and L.H. Allen, Jr., for their advice during this study. All of these contributors are with Agricultural Research Service, U.S. Department of Agriculture, Ithaca, N.Y.

This study was conducted in cooperation with the North Appalachian Experimental Watershed, Agricultural Research Service, U.S. Department of Agriculture, Coshocton, Ohio. This watershed provided the test area and the lysimeter data that were used in this analysis.

## CONTENTS

	<i>Page</i>
Summary .....	1
Introduction.....	1
Energy balance method .....	2
Aerodynamic approach .....	2
Equations for potential evapotranspiration .....	3
Limitations of meteorological methods .....	4
Experimental procedure.....	5
Variation of D and $z_0$ .....	5
Error analysis .....	5
Experimental results.....	8
Bowen ratio and aerodynamic methods .....	8
Combination formula.....	12
Discussion ... .....	15
List of symbols .....	17
Literature cited .....	19
Appendix A—Propagation of errors.....	21
Aerodynamic equation .....	22
Stability correction .....	22
Combination equation for potential ET .....	23
Appendix B—Instrumentation and data reduction.....	24
Lysimeter .....	24
Wind profile measurement and data reduction .....	24
Wet- and dry-bulb air temperature instrumentation .....	25
Description of other temperature measurement and data reduction .....	28
Description of radiation measurement and data reduction .....	28
Appendix C—Average hourly profile data .....	31
Appendix D—Average hourly evapotranspiration .....	50

Trade names and the names of commercial companies are used in this publication solely to provide specific information. Mention of a trade name or manufacturer does not constitute a guarantee or warranty of the product by the U.S. Department of Agriculture or an endorsement by the Department over other products not mentioned.

# ESTIMATING EVAPOTRANSPIRATION UNDER NONHOMOGENEOUS FIELD CONDITIONS<sup>1</sup>

By

Leslie H. Parmele and Earl L. Jacoby, Jr.<sup>2</sup>

## SUMMARY

Detailed micrometeorological measurements were made during selected days throughout 1969 by using weighing lysimeter on an adjacent watershed that had been planted with corn in order to test the application of commonly used meteorological methods of estimating evapotranspiration under conditions of rolling terrain. The experimental site was selected on a watershed that had a slope of 13 percent and that consisted of rolling-surface topography located in the U.S. Department of Agriculture's North Appalachian Experimental Watershed, Oshocon, Ohio.

With average hourly data being used, the Bowen ratio energy budget method proved superior to the ability-adjusted aerodynamic methods in comparing hourly lysimeter flux rates.

The Bowen method appears to be capable of

accurately estimating actual evapotranspiration under natural field conditions where fetch and surface homogeneity is less than ideal. Hourly computations in the combination equation for potential evapotranspiration agreed with the lysimeter for bare soil and for corn 75 centimeters high.

However, using the log profile wind function in the combination equation was unsatisfactory for corn at its full height of 240 centimeters unless the roughness length parameter ( $z_0$ ) was adjusted as a calibration term. An unusually low value for  $z_0$  of 1.0 centimeter resulted in the best fit of the combination equation with lysimeter flux rates for corn higher than 75 centimeters. Techniques were presented for making probable-error analysis of evapotranspiration estimates through meteorological methods.

## INTRODUCTION

The evaporation from bare soils and the evapotranspiration from vegetated surfaces have been studied in detail using meteorological methods capable of providing accurate, short-period flux rates. Under ideal conditions, meteorological methods have been highly successful in providing detailed information on the vapor transfer processes.

However, these methods have not been tested adequately for the nonhomogeneous surfaces, soils, and microclimatic conditions encountered in many natural situations apart from the ideal infinite fetch and short-growing, well-watered crops that characterized most past verification studies. Experimental studies are needed to test the

<sup>1</sup>Contributed by the Northeast Watershed Research Center, Agricultural Research Service, U.S. Department of Agriculture, University Park, Pa., in cooperation with the Agricultural Experiment Station, Pennsylvania State University.

<sup>2</sup>Formerly agricultural engineer with the Northeast Watershed

Research Center, Agricultural Research Service, U.S. Department of Agriculture, University Park, Pa., and hydrologic technician, Northeast Watershed Research Center, Agricultural Research Service, U.S. Department of Agriculture, Klingerstown, Pa.

application of meteorological theory against the realities of evapotranspiration from the nonideal cropped surfaces that are more commonly encountered in agricultural practices.

Thus, the available meteorological methods should be tested under the realities of evapotranspiration from cropped and heterogeneous surfaces. The instrumentation requirements and assumptions basic to a given model can be verified by comparing computed results against an independent measure, preferably an accurate weighing lysimeter. The purpose of this publication is to present such experimental results under less-than-ideal site conditions.

### Energy Balance Method

One of the most promising meteorological methods available is an energy balance approach known as the Bowen ratio method (2).<sup>3</sup> The Bowen ratio, defined as the ratio of sensible heat flux (H) to latent heat flux (E), can be derived by dividing the eddy transport equation for sensible heat flux by that for latent heat flux

$$B = \frac{H}{E} = \frac{c_p P K_h (\partial T / \partial Z) \rho}{L e K_v (\partial e / \partial Z) \rho} \quad (1)$$

Assuming  $K_h = K_v$ , an approximation of B can be obtained by using a finite difference form:

$$B = \frac{c_p P}{L} \frac{(\Delta T)}{(\Delta e)} = \gamma \frac{(\Delta T)}{(\Delta e)} \quad (2)$$

where T and e are temperature and vapor pressure measured over the same height interval just above the vegetation or bare soil surface.

Estimates of E using the Bowen ratio approach are then calculated from.

$$E = \frac{R_n + G}{1 + B} \quad (3)$$

where  $R_n$  and G are the measured net radiation and soil heat flux rates. Equation 3 has been used to measure evaporation from homogeneous surfaces, assuming that no horizontal divergence of fluxes occurs between the levels of measurement and the evaporating surface.

The advantages and disadvantages of the Bowen method are discussed in other sources (5, 26). Lanner (27) reported close agreement between calculated evapotranspiration rates and lysimeter-measured values in a humid climate with a well-watered crop. In warm, arid regions, the Bowen method has been used by Fritsch (5, 6) successfully to determine the evaporative flux for short periods. These determinations can also be made for longer period values.

### Aerodynamic Approach

Aerodynamic approaches for estimating total water vapor flux from an evaporating surface depend on assumptions that are well documented in the literature cited (23, 26, 28, 32). Generally, these assumptions are:

- Mean wind speed varies logarithmically with height.
- Eddy shear stress is constant with height
- Eddy diffusivity for water vapor ( $K_v$ ) is equal to that for momentum ( $K_m$ ).

The equation based on these assumptions most commonly used in evaporation measurement under adiabatic conditions is:

$$E = \frac{\epsilon L \rho k^2 (e_1 - e_2) (u_2 - u_1)}{[\ln (Z_2 - D / Z_1 - D)]^2} \quad (4)$$

Equation 4 permits the prediction of latent heat flux rates from carefully measured profiles of vapor pressure (e) and horizontal wind velocity (u). The displacement height (D) ( $D = z_0 + d$ ) must be subtracted from the height value (Z) as measured from ground surface. This adjustment is necessary because, as figure 1 shows, where there is a tall, aerodynamically rough vegetation, the logarithmic wind-profile distributions on which equation 4 is based are displaced upward from the ground surface. The parameter  $z_0$  is a constant that is used to define the roughness characteristics of a given surface. It is determined by graphically extrapolating the logarithmic profile of measured velocities downward to where wind speed theoretically should be zero. The parameter d is the height of the  $z_0$  reference plane displacement.

The above approach is valuable only under near-adiabatic conditions. When surface heating or cooling produces a nonadiabatic temperature profile, the straight-line relationship of u versus  $\ln (Z - D)$  no longer holds, especially under low-wind conditions.

<sup>3</sup>italic numbers in parentheses refer to literature Cited, p. 19.

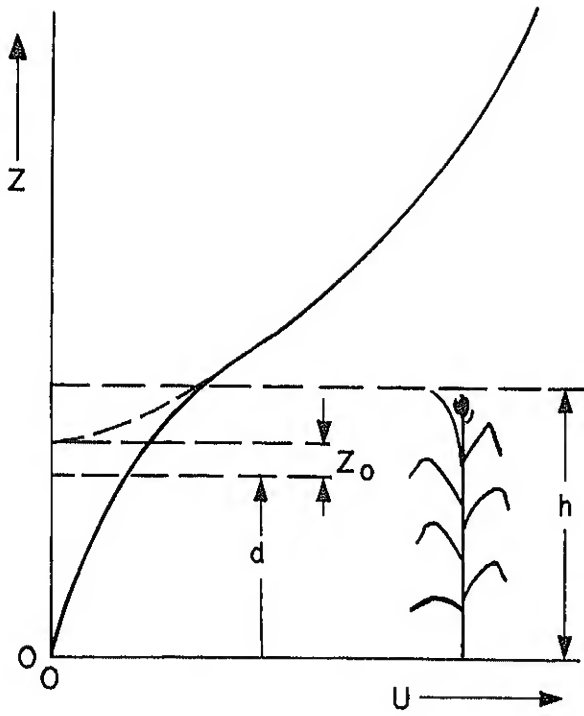


Figure 1.—Schematic representation of wind velocity distribution ( $U$ ) with height above ground ( $Z$ ) in a plant community with height ( $h$ ). Wind velocity distribution is logarithmic with height above plants, and exponential with height within the plant community. Logarithmic profile extrapolation downward to zero wind speed ( $u = 0$ ) is indicated by a dashed curve with an intercept of  $d + Z_0$  (1/2).

Under conditions of appreciable temperature gradients because of surface warming or "free convection," equation 4 will underestimate the flux rate since the added effect of buoyant turbulence has not been considered. Similarly, temperature inversions over cold surfaces damp out turbulent exchange, causing equation 4 to overestimate exchange rates.

Several means have been proposed to adjust for the influence of temperature gradients (23). One approach is to incorporate a form of diabatic correlation function that can then be related empirically to a stability parameter.

The form of the relationship normally used is:

$$\psi = (1 - b R_1)^{-1/4}, \quad (5)$$

where  $R_1$  is the gradient Richardson number, a commonly used stability parameter. This non-dimensional number ( $R_1$ ) is a quantitative ratio of thermal turbulence effects, compared with frictional turbulence effects that have the form of

$$R_1 = \frac{g}{T_{\text{abs}}} \frac{(\partial T / \partial Z)}{(\partial u / \partial Z)^2} \quad (6a)$$

where  $g$  is the constant of gravity, and where  $T_{\text{abs}}$  is the absolute temperature. Equation 6a can be approximated by

$$R_1 = \frac{(g(Z_2 - Z_1) / T_{\text{abs}})}{[(T_2 - T_1) / (u_2 - u_1)^2]} \quad (6b)$$

and is applicable to a mean height ( $z$ ) between  $z_1$  and  $z_2$ , where  $\Delta T$  and  $\Delta u$  are measured.

The coefficient  $b$  in equation 5 must be determined experimentally. Panofsky, Blackadar, and McVehil (16) recommended a value of 18 after analysis of several data sources. With this  $b$  value, equation 5 is commonly called the "KEYPS" profile.

Another empirical diabatic profile correction developed at Davis, Calif. (20) is:

$$\psi = (1 \pm 50 R_1) \pm 1/4, \quad (7)$$

where the -50 and -1/4 apply in the unstable case, and the +50 and +1/4 apply in the stable case.

Equation 4 can be modified by introducing the diabatic correction function  $\psi$ . Thus, to correct evaporation flux calculations for all conditions of thermal stability, the following equation (26) is used

$$E = \frac{\epsilon L \rho k^2 (e_1 - e_2) (u_2 - u_1)}{[\ln (Z_2 - D) (Z_1 - D)]^2 (\psi)^2} \quad (8)$$

### Equations for Potential Evapotranspiration

Potential evapotranspiration is a micrometeorological concept that is proposed to be the actual evapotranspiration under conditions of freely available water and that is intended to provide a base line for computing *actual* evapotranspiration as a fraction of *potential* evapotranspiration.

The combination method for estimating potential evaporation was developed by Penman from both energy balance and aerodynamic transport equations (17). Much attention has been given to the derivation and application of the combination method and its various versions in estimating potential evaporation. Many sources are available for more detailed information (1, 3, 10, 11, 18, 24, 27, 28, 31).

Van Bavel (31) described the development, limitations, and adequacy of the Penman combination concept in considerable detail. More recent formulations of the combination equation are an improvement over the original Penman versions in that they contain fewer empirical constants or functions. Basically, the current accepted equation (31) is:

$$E_p = \frac{s}{s + \gamma} \left[ (R_n + G) + \frac{\rho c_p}{s} \frac{1}{r_a} (e_s - e_a) \right] \quad (9)$$

where  $e_s$  and  $e_a$  are the saturated and actual vapor pressure of the air at height  $Z_a$  above the given surface. In contrast with the original Penman formula:

- Net radiation ( $R_n$ ) is actually measured, instead of relying on an empirical estimate of this parameter.
- Correction is made for soil heat flux ( $G$ ) that had been previously omitted.
- $r_a$  is derived from the log wind-profile theory of Thornthwaite and Holzman (29) and referenced from the displacement height ( $D$ ).

$$r_a = \frac{\left[ \ln \left( \frac{Z \cdot D}{z_0} \right) \right]}{k^2 u_z} \quad (10)$$

- An empirical constant is not included as an adjustment for crop wetness or stomatal control.
- Vapor pressure at the evaporating surface is equal to the saturation vapor pressure at surface temperature.

The combination method for potential ET requires these assumptions:

1. The eddy diffusivity for momentum equals that for heat and water vapor,  $K_m = K_h = K_v$ .
2. The air temperature at point of measurement can be substituted without undue error for the average of the air and surface temperatures in evaluating

$$\gamma (S/S + \gamma)$$

By referring to equation 9, one can apply a method based on potential evapotranspiration to any surface with freely available water. The only differences in evaporation from a water surface, from bare wet soil, and from a well-watered vegetative surface would be due to variations in surface radiative properties and

in aerodynamic transport characteristics of the layer through which water vapor moves away from the evaporating surface, assuming that vapor pressure ( $e_s$ ) is at saturation.

In this form, no provision is made for differences in stomatal characteristics making one crop "wetter" than another, even when well watered. Tests of combination equations 9 and 10 for open water, wet bare soil, and well-watered alfalfa (a "wet" crop) showed excellent agreement on both an hourly and on a daily basis under a variety of physical conditions in Phoenix, Ariz. (31).

### Limitations of Meteorological Methods

For routine field conditions, these meteorological methods could be impractical because of measurement difficulties and inaccurate because of the failure of the theoretical model to fit less-than-ideal conditions of a horizontally uniform, two-dimensional surface. Peterson (19) discussed the problems associated with flows encountered in heterogeneous terrain. His predictions indicate that the standard techniques for estimating the eddy diffusivities or exchange coefficients may lead to unacceptable errors in estimating the vertical fluxes of momentum, heat, and moisture over a heterogeneous surface. Many agricultural and natural surfaces simply cannot be regarded as homogeneous.

Surface nonhomogeneity may not only affect the ratios of ( $K_h/K_m$ ) and ( $K_h/K_v$ ), but also may create sampling problems in measurement of gradients and other terms with the required accuracy.

When sensors are elevated to obtain better spatial sampling and maximum possible vertical differences, the profile measurements of wind, temperature, and vapor concentration are affected more and more by surfaces further upwind and less by the surface immediately below the sensor. At some point the measured profile gradients are not representative of processes that are occurring on the reference surface. Thus, a buffer area of the same type as the reference surface is required to reduce the possibility of divergence errors in measuring the vertical fluxes. This buffer area is referred to as "fetch" and is the minimum upwind distance to a significantly different surface from the point of measurement. Nonhomogeneity influences fetch requirements in that the required height-to-fetch ratios should be 1 to 50 for minor discontinuities and at least 1 to 100 or 1 to 200 if the discontinuity is severe (26). These "ideal" fetch requirements are difficult if not impossible to satisfy under many field situations.

## EXPERIMENTAL PROCEDURE

The experimental site was developed on watershed 109 at the U.S. Department of Agriculture, North Appalachian Experimental Watershed, Coshocton, Ohio. The watershed (fig. 2) lies just below the crest of a major ridge that extends through the area and that has an average slope of 13 percent in an eastward direction. Agricultural fields border the north, south, and west sides of the watershed; gravel roads traverse the north and east sides. The rolling terrain is far from an ideal homogeneous surface as required for the classical type of micrometeorological studies. At the center of the watershed a micrometeorological sampling site for temperature, humidity, and wind profiles was established. Most energy budget data and further profile measurements of humidity, temperature, and wind were obtained at lysimeter Y102C, located 200 feet north of the central watershed sampling site. The instrument trailer that housed the recording equipment was parked on the boundary of the field approximately 100 feet northwest of the lysimeter site.

The entire watershed, including lysimeter, was planted in corn on May 1, 1969, in 42-inch rows generally oriented in a southwest-northwest direction parallel to the contour of the field. The prevailing winds in the area are from the southwest and provide the best fetch conditions for the two sites.

Complete micrometeorological measurements were made at the lysimeter site on May 2 and 22, June 26, July 24, August 27, and October 14 and 16, 1969. Micrometeorological measurements were not made at the midwatershed site during the first two test periods. The midwatershed profile data on June 26 were inaccurate because of instrumental difficulties, so that data at the midwatershed site were available only on July 24 and afterward. A summary of conditions for each data is given in table 1.

The corn was harvested on October 15 and the soil disked to prepare for winter wheat planting. Thus, the data on October 16 were obtained on bare soil partly covered with litter from cornstalks.

A complete description of the instrumentation and data-reduction techniques can be found in appendix B. A listing of the average hourly micrometeorological data is listed in appendix C.

### Variation of D and $Z_0$

The determinations of D and  $Z_0$  that were used in equations 4 and 10 are two of the most demanding measurements in the profile methods, because each depends on accurate measurement of the *second-order* properties of the profile. D and  $Z_0$  must be determined under adiabatic situations because lack of stability in these parameters may introduce errors (15). Since D and  $Z_0$  of cropped surface may change several centimeters with varying wind speed (12, 30), errors may also arise from assuming that D and  $Z_0$  are constant for a given surface.

Mukammal (15) has indicated that the determination of D is very sensitive to small errors in wind speed measurement. He observed that under a given set of conditions, an increase of only 1.0 centimeter per second in the average speed of the middle level of a three-level wind system increased D by 50 percent, from 40 centimeters to 60.

### Error Analysis

The meteorological estimates of E were basically indirect measurements; that is, the unknown (E) was determined by using an equation that related it to some other measurable quantities such as radiation, temperature, wind speed, and vapor pressure. Each measured variable had a certain standard deviation of the mean or probable range of error. Thus, each computed value of E had some uncertainty associated with it. The magnitude of the uncertainty depended both on the magnitude of the errors in each of the measured variables and on the nature of the equation itself.

Because of the problems in evaluating D and  $Z_0$  accurately, the probable maximum error for each was assumed to be  $\pm 25$  percent of the absolute value for use in error analysis. The magnitude of these possible errors appeared reasonable in light of the preceding discussion.

A probable uncertainty or error in each calculated hourly value of E was evaluated by using procedures outlined in appendix A. All estimates of possible error were based on probable measurement errors for each variable (table 2). The estimated range or probable uncertainty in a particular E estimate assumed that all sensors and recording systems were operating within their accepted limits and that no error was introduced in the data-reduction process.

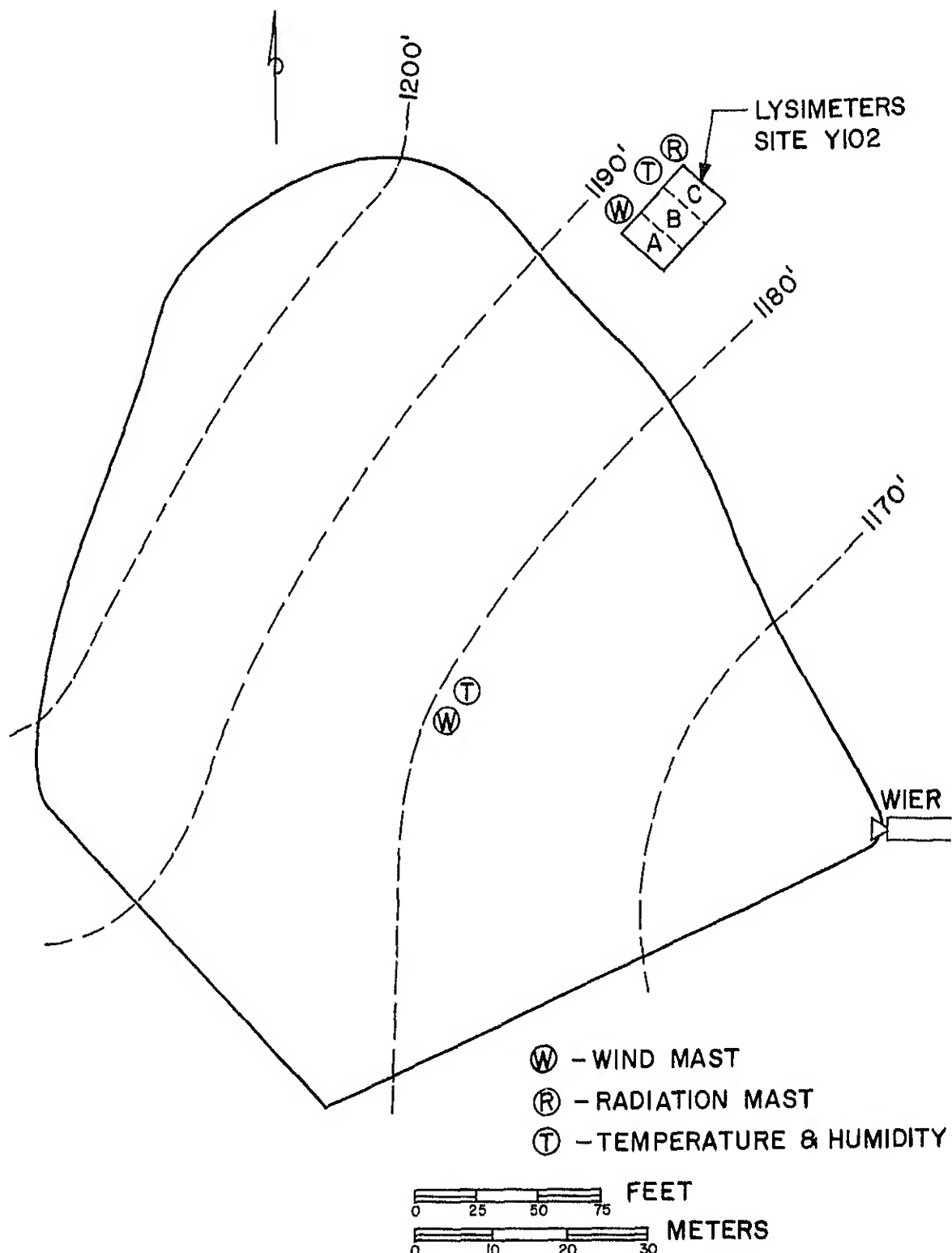


Figure 2.—Map of field experimental site at Coshocton, Ohio, showing location of instrument trailer, lysimeter Y102, and micrometeorological sensors.

Table 1 -A summary of conditions and measurements on days of experimental observations at lysimeter Y102C and watershed 109, Coshocton, Ohio

Date	Time (EST)	Soil conditions	Accumulated E (lysimeter)	Accumulated precipitation	Cover and crop height (h)	Av u (cm/s) direction	General weather conditions	Measurements	Height of $\Delta e$ and $\Delta T$	Length of fetch
									cm	m
5/2/69	04-22	Dry and loose on surface	0	0	Bare soil,	250 (SW)	Clear and warm.	Lysimeter Y102C, $R_n$ , G, $\Delta e$ , $\Delta T$ , $\Delta u$ .	10 and 100 D = 0 $z_0 = 0.1$	150
5/22/69	04-22	Surface moist	5.1	6.1	General bare soil corn corn h = 5.	150 (N)	Overcast and cold 0.05" rain @ 1200 EST. $\Delta T$ , $\Delta u$ . EST.	Lysimeter Y102C, $R_n$ , G, $\Delta e$ , $\Delta T$ , $\Delta u$ .	10 and 100 D = 0 $z_0 = 0$	15
6/26/69	04-22	Wet soil saturated to field capacity.	15.2	20.9	Corn almost complete cover h = 75.	200 (SW)	Clear and warm.	Lysimeter Y102C, $R_n$ , G, $\Delta e$ , $\Delta T$ , $\Delta u$ .	150 and 250 $z_0 = 2.0$	150
7/24/69	04-22	Wet	26.7	39.4	Corn h = 240.	100 (SW)	Clear with haze, rain @ 1500 EST	Lysimeter Y102C, $R_n$ , G, $\Delta e$ , $\Delta T$ , $\Delta u$ .	250 and 350 $z = 15.0$	150
8/27/69	05-23	Surface dry, sub-surface moist.	42.0	52.0	Corn h = 240.	100 (N-S)	Clear, light, variable wind.	Lysimeter Y102C, $R_n$ , G, $\Delta e$ , $\Delta T$ , $\Delta u$ . Watershed 109 $\Delta e$ , $\Delta T$ .	250 and 350 $z_0 = 20.0$	15 to 150 50 to 75
10/14/69	05-20	Dry	---	57.5	Corn ready to harvest h = 130.	150 (NW)	Overcast and cool.	Lysimeter Y102C, $R_n$ , G, $\Delta e$ , $\Delta T$ , $\Delta u$ . Watershed 109, $R_n$ $\Delta e$ , $\Delta T$ , $\Delta u$ .	150 and 250 $z_0 = 8.0$	15 to 100
10/16/69	07-19	Dry, surface moist.	---	57.7	Bare soil with litter.	500 (SW)	Partly cloudy and cool.	Lysimeter Y102C, $R_n$ , G, $\Delta e$ , $\Delta T$ , $\Delta u$ . watershed 109, $R_n$ , $\Delta e$ , $\Delta T$ , $\Delta u$ .	25 and 100 $z_0 = 0.1$	150

Table 2—Recording and sensor accuracy of micrometeorological variables for use in probable-error analysis

Variable	Accuracy of		Probable measurement error
	Recorder	Sensor	
$R_n$	± 0.01 langley/min	± 0.02 langley/min	± 0.02 langley/min
G	± .01 langley/min	± .02 langley/min	± .02 langley/min
$T_{abs}$	± 35° C	± 10° C	± 40° C
$\Delta T$	± .02° C	± .02° C	± .03° C
$\Delta T$ (wet bulb)	± .02° C	± .02° C	± .03° C
$e_s, e_a$	---	---	± 60 mbar
$\Delta e$	---	---	± .10 mbar
$(e_s - e_a)$	---	---	± .80 mbar
u	± 4.5 cm/s	---	± 4.5 cm/s
$\Delta u$		---	± 6.4 cm/s
$z_0$	Assume 25% of $Z_0$	---	---
D	Assume 25% of D	---	---

## EXPERIMENTAL RESULTS

### Bowen Ratio and Aerodynamic Methods

A comparison of hourly estimates E using the Bowen ratio and aerodynamic equations with the lysimeter value for May 2 is shown in figures 3 and 4, and for June 26 in figures 5 and 6, respectively. Both days were characterized by clear skies. Wind was from the south-southwest for most of the day, with speeds ranging from 100 to 300 centimeters per second. This direction provided the most ideal fetch conditions at the lysimeter test area.

On May 2, measurements were made over bare, dry soil. As a result of the solar heating of the bare soil, measurements indicated strong temperature and humidity gradients, and the soil surface temperature reached 40° C during midday. Bowen ratios (B) ranged from 1.2 to 1.9 during daylight hours, indicating that most of the radiant energy was being transferred into sensible heat.

The large negative Richardson numbers that prevailed during the measurements on May 2 resulted in a large diabatic correction to the aerodynamic equation (8). Evaporation computed from the simple uncorrected logarithmic equation (4) averaged 50 percent less than those obtained with equation 8. This required the largest diabatic correction on any of the 7 test days. The closeness of the Bowen ratio estimate and the aerodynamic estimates using "KEYPS" correction was encouraging. There appeared to be a tendency for the

aerodynamic equation with the Davis adjustment to overcompute E on this day.

The range of probable error on May 2 was very small for both aerodynamic and Bowen ratio estimates, ranging from ± 0.01 to ± 0.02 langley per minute. The probable error for the Bowen ratio estimate was shown to increase considerably at 1800 hours to a range of ± 0.07 langley per minute.

The run of June 26 was made over corn 75 centimeters high following a week of heavy rains that had brought the soil to field capacity. This day was a marked contrast to conditions on May 2, in that the temperature profiles were very close to adiabatic during most daylight hours. Practically all the net radiation went into latent heat flux, with Bowen ratio values (B) ranging from -0.13 to 0.20 during daylight hours. Because of the low Richardson numbers, (-0.01 to +0.01), only a slight diabatic correction ( $\psi^2$ ) was necessary for the aerodynamic equation, ranging from 0.90 to 1.0, maximum.

Evaporation flux rates computed by aerodynamic and Bowen ratio methods on June 26 at the lysimeter site were compared with the measured lysimeter values (figs. 5 and 6). The Bowen ratio method agreed closely with the lysimeter data, while the aerodynamic method provided slightly lower values during the hours 1100 to 1600.

Except for a couple of hours, the Bowen ratio estimate was generally within the probable error

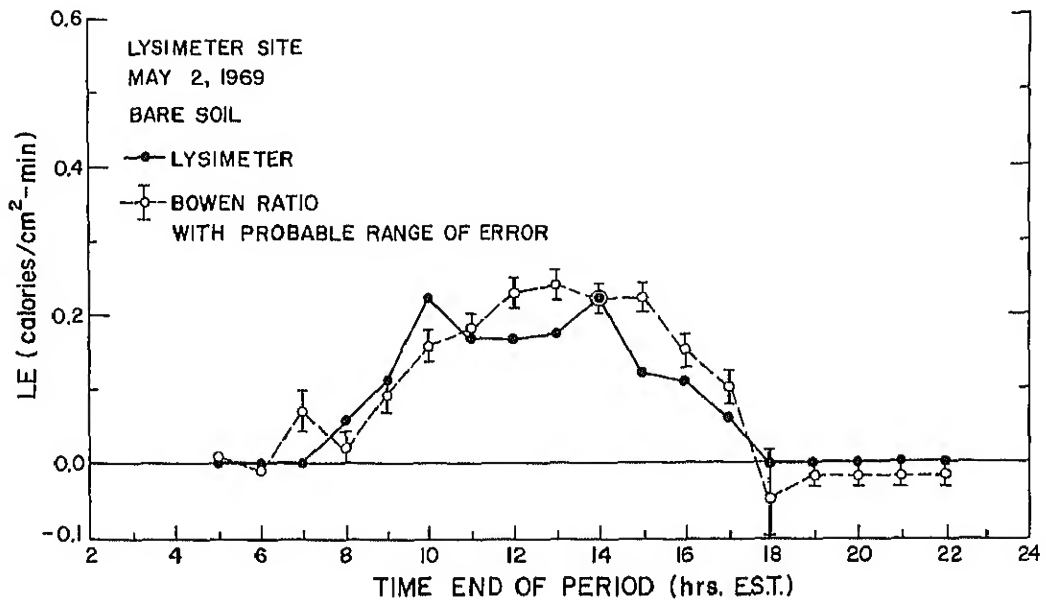


Figure 3.—Hourly evaporative flux from bare soil obtained on May 2, 1969, from weighing lysimeter Y102C at Coshocton, Ohio and calculated with Bowen ratio method showing range of probable error in estimating LE.

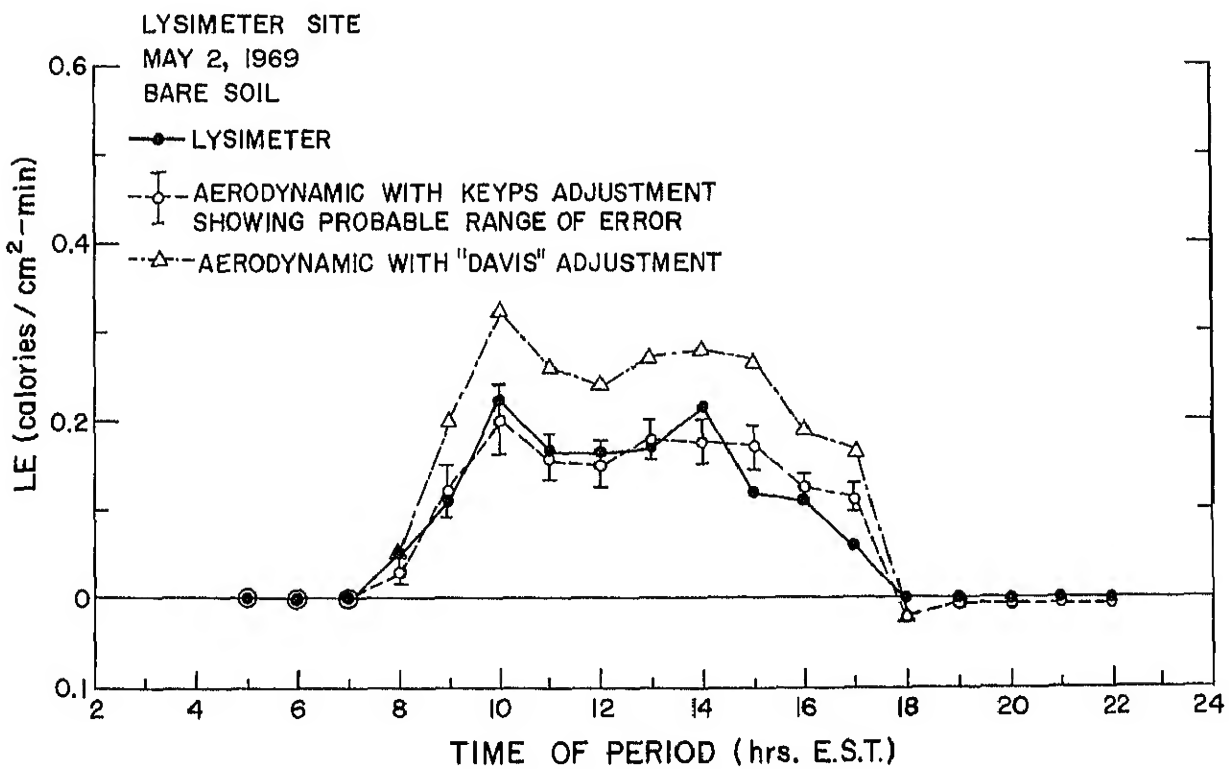


Figure 4.—Hourly evaporative flux from bare soil obtained on May 2, 1969, from weighing lysimeter Y102C at Coshocton, Ohio, and calculated with adjusted aerodynamic methods showing range of probable error in estimating LE.

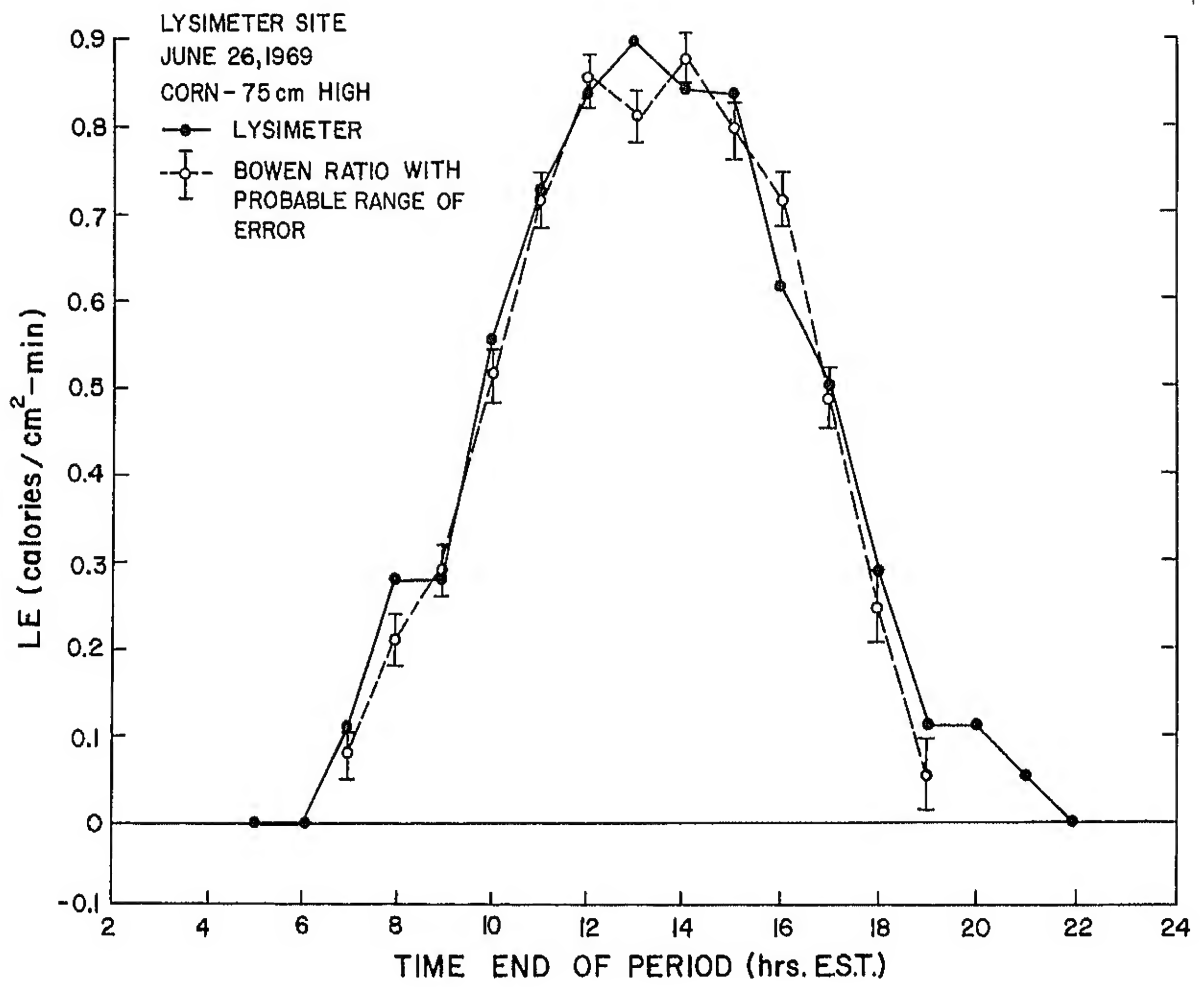


Figure 5 —Hourly evaporative flux from corn (75 cm) obtained on June 26, 1969, from weighing lysimeter Y102C at Coshocton, Ohio, and calculated with Bowen ratio method showing range of probable error in estimating LE.

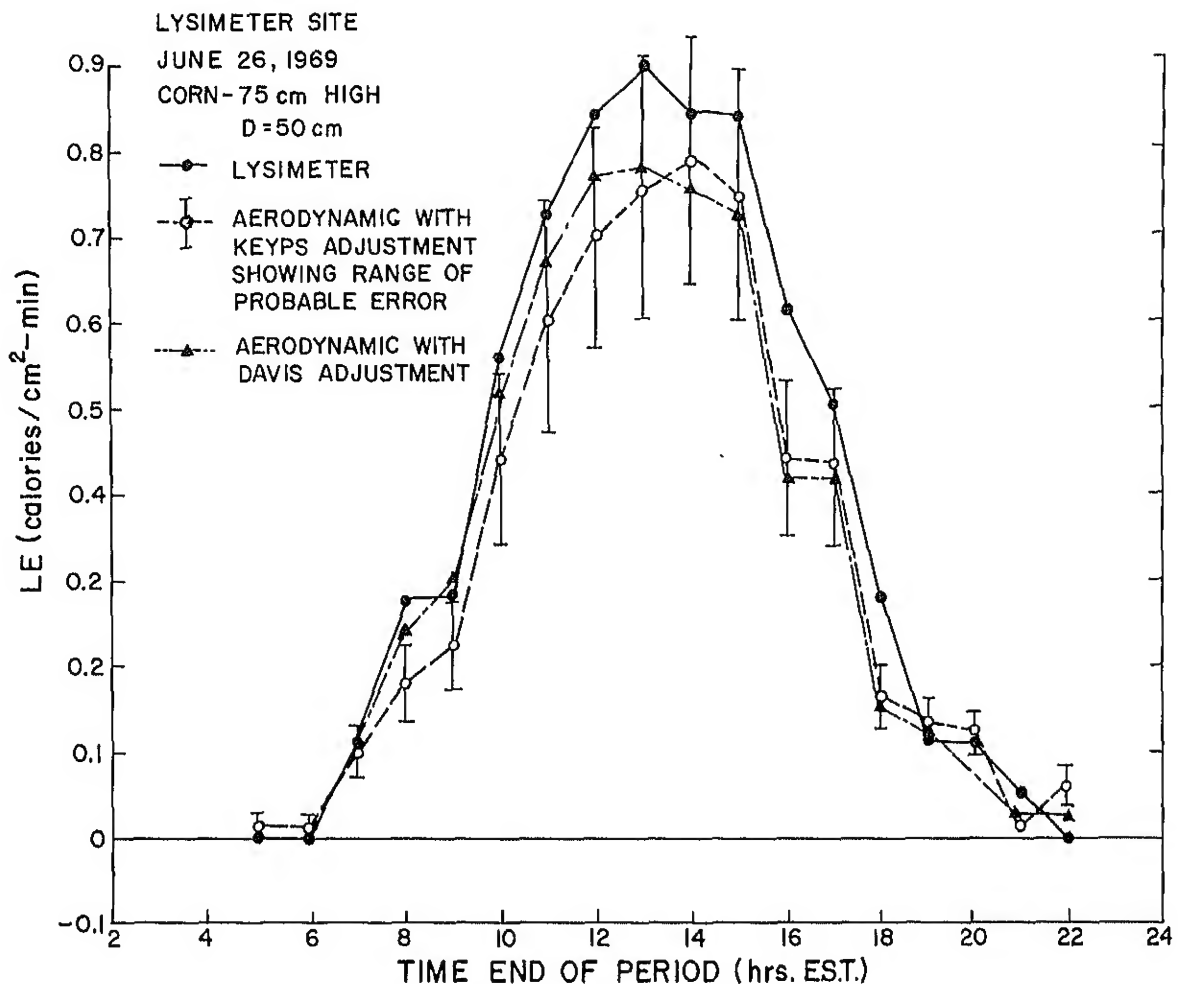


Figure 6 --Hourly evaporative flux from corn (75 cm) obtained on June 26, 1969, from weighing lysimeter Y102C at Coshocton, Ohio, and calculated with adjusted aerodynamic methods showing range of probable error in estimating LE

range of 0.03 langley per minute from the lysimeter value. The range of probable error for the aerodynamic estimate was very large from 1100 to 1600 hours, ranging from  $\pm 0.10$  to  $\pm 0.15$  langley per minute on an hourly basis. Reliability in the aerodynamic estimate of E was greater during the early morning and late evening hours.

D was assumed to be accurate within  $\pm 25$  percent of the "true" value for use in the error analyses. On June 26th, with  $h = 75$  centimeters and  $D = 50$  centimeters, this probable error in D would be  $\pm 12$  centimeters. If it were possible to estimate D without error, the range of probable uncertainty in the aerodynamic estimate of E would be reduced to 0.06 langley per minute from 1100 to 1600 hours.

Thus, the large uncertainty in the aerodynamic estimate can be traced partly to the uncertainty in the estimate of D. Confidence could be improved by

increasing the sampling heights so that D is small, relative to  $Z_2$  and  $Z_1$ . However, if this is done, the profile measurements may not be representative of the processes occurring on the given surface.

The comparisons described above are for the 2 test days considered most ideal. Conditions for the other days were often far from ideal. A summary of total daylight vapor flux (E) by the various methods for all periods is given in table 3 and is listed in appendix D along with the lysimeter values for the hourly periods.

The Bowen ratio estimate was within 10 percent of the total lysimeter E measured on five of the seven cases and within 20 percent on the last 2 test days. The difference for the total E on these days is well within the accuracy of the meteorological and lysimeter measurements.

The results obtained with the aerodynamic estimates were more variable. Only in a few cases did

Table 3.—A comparison of observed lysimeter  $E$ , with  $E$  computed hourly by Bowen ratio and aerodynamic methods with daylight total added

Date	Time (EST)	E Lysimeter Y102C	Bowen ratio		Aerodynamic equation			Fetch height ratio <sup>1</sup>
			Equation 3	Probable error	Davis adj. equation 8 and 5	Keyps adj equation 8 and 7	Probable error Keyps	
Mm								
Lysimeter site								
5/2/69	7-18	1.42	<sup>2</sup> 1.40	$\pm$ 0.08	2.42	<sup>2</sup> 1.57	---	150
5/22/69	12-20	1.23	<sup>2</sup> 1.33	$\pm$ .11	<sup>2</sup> 1.27	<sup>2</sup> 1.29	---	15
6/26/69	5-22	7.06	<sup>2</sup> 6.74	$\pm$ .12	<sup>2</sup> 6.35	<sup>3</sup> 5.90	$\pm$ 0.37	50
7/24/69	6-16	3.81	<sup>2</sup> 3.46	$\pm$ .12	<sup>3</sup> 3.31	2.30	$\pm$ .56	45
8/27/69	6-23	4.60	<sup>2</sup> 4.38	$\pm$ .16	2.78	1.96	$\pm$ .17	5-45
10/14/69	8-18	.92	.60	$\pm$ .08	.49	.38	$\pm$ .04	6
10/16/69	8-17	1.10	<sup>3</sup> .90	$\pm$ .16	<sup>2</sup> 1.22	<sup>2</sup> 1.20	$\pm$ .01	150
Watershed site								
7/24/69	6-16	3.81	<sup>3</sup> 3.20	$\pm$ .11	5.76	<sup>2</sup> 3.78	$\pm$ 1.08	20
8/27/69	6-23	4.60	<sup>3</sup> 4.10	$\pm$ .21	3.05	2.10	$\pm$ .37	15-20
10/14/69	8-18	.92	<sup>2</sup> .94	$\pm$ .17	<sup>3</sup> 1.30	<sup>3</sup> 1.10	$\pm$ .08	40
10/16/69	8-17	1.10	.46	$\pm$ .5	.08	.07	$\pm$ ---	75

<sup>1</sup>Ratio of minimum upwind distance from sampling site of surface being measured to height of highest sampling point in profile measurements used in computations.

<sup>2</sup>Computed  $E$  within  $\pm 10$  percent of lysimeter  $E$ .

<sup>3</sup>Computed  $E$  within  $\pm 20$  percent of lysimeter  $E$ .

the computed flux rates closely agree with the lysimeter or Bowen ratio estimates of  $E$  after crop height had exceeded 75 centimeters. Between May 2 and July 24, the probable range of uncertainty increased from  $\pm 0.07$  to  $\pm 0.56$  langley per minute, as  $D$  increased because of crop growth from 0 to 150 centimeters. The total flux estimate on July 24 would have had an uncertainty of  $\pm 0.24$  langley per minute if it could be assumed that "D" had been measured without error. Thus, a major source of error in the aerodynamic method appears to be the uncertainty in the measurement or approximation of the displacement height  $D$ .

A large variation occurred in the aerodynamic and Bowen ratio estimates at the lysimeter site on August 27 and again on October 14. This failure can be related to poor fetch conditions; light, variable winds arose on both days. On October 14, the watershed site was better suited in regard to wind direction and fetch. The results at the watershed site showed that all three estimates agreed on this day. In contrast, on October 16 and under heavy winds, the watershed site failed to provide any meaningful estimates, whereas the lysimeter site with a longer fetch closely agreed on all three estimates. Generally, the Bowen ratio estimates of  $E$  provided reasonable

accuracy when the fetch/height ratio was in the range of 20 to 1 through 50 to 1, except for October 16 when, for bare soil, a fetch of 75 to 1 was inadequate. A fetch/height ratio of greater than 50 to 1 appears necessary for successful application of aerodynamic techniques.

#### Combination Formula

Four days—May 22, June 26, July 24, and August 27—were considered to have met the requirements of nonlimiting water supply necessary to satisfy the definition of potential evapotranspiration. Latent heat flux was computed hourly for each day from equation 9 using  $Z_0$  as determined from wind-profile analysis. The results for two of these days are plotted in figures 7 and 8. On June 26, the estimated value of  $E_p$  was close to  $E$ , but about 10 percent greater than the amount as measured by the lysimeter. The range of probable error in the  $E_p$  was generally  $\pm 0.04$  to  $\pm 0.08$  langley per minute, assuming an uncertainty in  $Z_0$  of 0.5 centimeter, with  $Z_0$  equal to 2.0 centimeters. Thus considering the range of uncertainty, hourly  $E_p$  estimates agreed with the lysimeter except, perhaps, from 1400 to 1700.

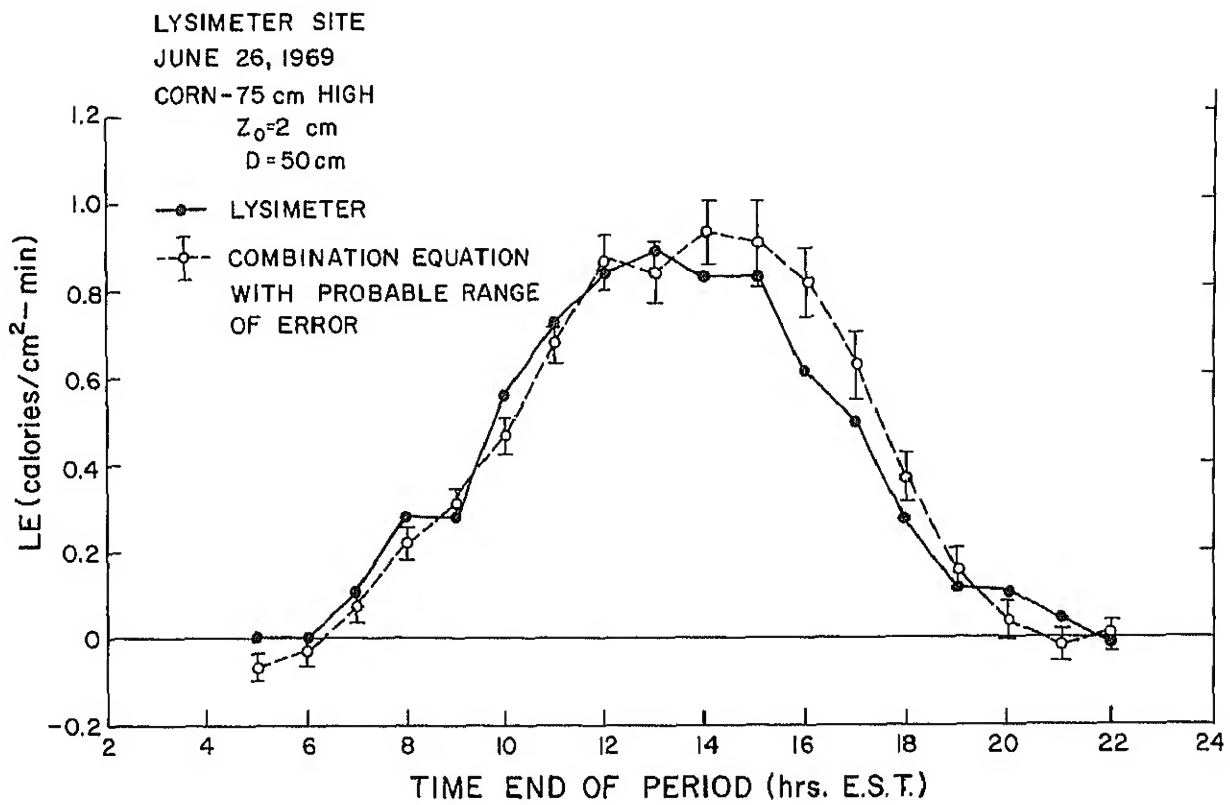


Figure 7.—Hourly evaporative flux from corn (75 cm) obtained on June 26, 1969, from weighing lysimeter Y102C at Coshocton, Ohio, and calculated potential ET by combination equation showing range of probable error in estimating ET.

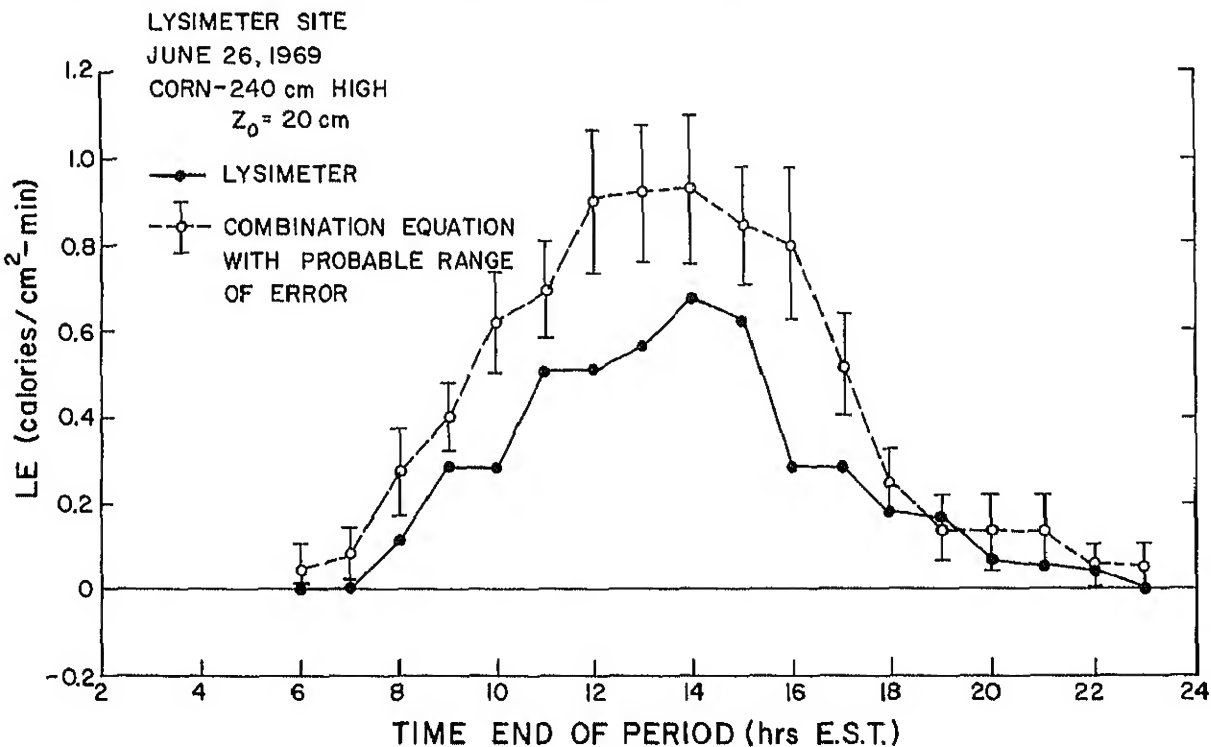


Figure 8.—Hourly evaporative flux from corn (240 cm) obtained on August 27, 1969, from weighing lysimeter Y102C at Coshocton, Ohio, and calculated potential ET by combination equation showing range of probable error in estimating ET.

In contrast, the results for August 27 revealed an overestimation of  $E$  by more than 100 percent of the lysimeter value.  $E_p$  also exceeded net radiation by 10 to 15 percent from 1100 to 1600. The range of probable error ( $\pm 0.15$ ) was very large compared with the June 26 range in probable error ( $\pm 0.06$ ).

A summary of totalized daylight hourly values for each of the 4 days is given in table 4, column 2. Equation 9, using measured  $Z_o$  values, failed to predict  $E$  accurately once the corn had reached full height at 240 centimeters. On May 22, agreement between computed  $E_p$  and lysimeter flux rates for bare soil was excellent despite poor fetch conditions.

The value  $Z_o$  can be estimated as a function of crop height (26) by the equation.

$$Z_o = 0.058 h^{1.19} \quad (11)$$

The value  $Z_o$  could have been estimated on the basis of equation 11 rather than on the basis of a transposed value from the Ithica, N.Y., experiment previously mentioned or wind-profile analysis. Then, the values of  $Z_o$  would be 10 and 40 centimeters for crop heights of 75 and 240 centimeters, respectively. Used in equation 9 these  $Z_o$  values would greatly increase the difference between computed  $E_p$  and observed  $E$ . Thus, it was necessary to substitute the value from the Ithaca, N.Y., experiment because of the nonhomogeneous terrain at the Coshocton, Ohio, site.

In reference to the totalized daylight values given in table 4, the probable error in the period total for individual days increased considerably as  $Z_o$  rose

from 0.1 to 20 centimeters, assuming an uncertainty of  $\pm 25$  percent in the  $Z_o$  estimate. An absolute measure of  $Z_o$  would reduce the range of probability error to  $\pm 0.13$  millimeter per day or less for all 4 days. This uncertainty in the  $E_p$  estimate could account for some of the difference; however, it is doubtless not the only reason for the overcomputation of  $E$  on July 24 and August 27.

The log law for neutral profiles from which equation 10 was derived is recognized to be in error for diabatic situations. Tanner (26) suggests that the wind function (10) includes a diabatic convection factor similar to that used in the aerodynamic equation correction. However, if such a correction factor were applied to the 3 days in question, it would increase the error between estimated and observed lysimeter flux rates. Accounting for this disagreement would be easy by assuming that the surface was not a potential evaporation surface or that the measurements of the meteorological variables were not representative. The success of the Bowen ratio estimates invalidates this later argument.

If the surface is not evaporating at the potential rate, then computing the surface diffusion resistance ( $r_s$ ), which is a means of defining the degree of unsaturation of the crop and soil system, should be possible. When the energy balance of the crop and the aerodynamic resistance term are known,  $r_s$  can be calculated as a residual from the ratio of potential to actual evaporation (25).

$$r_s = r_a \left( 1 + \frac{\Delta}{\gamma} \right) \left( \frac{E_p}{E_{LYS}} - 1 \right) \quad (13)$$

Table 4.—*Observed lysimeter E during periods of adequate moisture supply, compared with potential evaporation ( $E_p$ ), computed hourly by combination equation with total for period*

Date	Time (EST)	E Lysimeter Y102C (1)	Equations 9 and 10 measured $z_o$ (2)	Probable error $z_o \pm 25\%$ (3)	Equations 9 and 10 assume $z_o = 1.0$ cm (4)	Penman version (5)	Measured $z_o$ (6)
		Mm	Mm	Mm	Mm	Mm	Cm
5/22/69	1200 to 2000	1.23	1.06	$\pm 0.07$	---	1.17	0.1
6/26/69	500 to 2200	7.06	7.85	$\pm .20$	7.14	6.78	2
7/24/69	600 to 1600	3.81	4.55	$\pm .28$	3.51	3.60	15
8/27/69	600 to 2300	4.60	8.14	$\pm .47$	4.87	5.03	20

<sup>1</sup>Computed  $E_p$  within  $\pm 10$  percent of lysimeter  $E$ .

<sup>2</sup>Computed  $E_p$  within  $\pm 20$  percent of lysimeter  $E$ .

Potential evaporation ( $E_p$ ) can be calculated from equation 9. When the measured  $Z_o$  values were used, the calculation of  $r_s$  provided hourly values from 0 to 0.8 second per centimeter for June 26, and from 0.5 to 2.5 seconds per centimeter for August 27 during daylight periods. These estimates for  $r_s$  appear reasonable, but there are no independent measures of  $r_s$  or soil water potential for comparison. Because of the high degree of recharge during this period (table 2), precipitation - measured evaporation), probably no soil moisture deficiency existed. Thus, water was not limiting, and potential conditions should be as valid on July 24 and August 27 as on June 26.

Jensen (9) and Rosenberg (21) both report failure of the combination equation 9 when using the aerodynamic term (10) proposed by Van Bavel (31). Jensen indicates that under arid conditions it is necessary to calibrate  $r_a$  by varying the  $Z_o$  value until the  $E_p$  estimate of equation 9 had agreed with a lysimeter measure. Sellers (22) has indicated that unreasonably high  $E$  estimates have been obtained by using simple logarithmic profile methods over tall crops. Van Bavel's verification of the modified combination equation (31) was limited to bare soil and alfalfa 25 to 30 centimeters high. The authors too

could find no reported applications of equation 9 to a tall crop such as corn, where an independent measure of  $E$  was available for verification.

Potential evaporation was recalculated for the 3 days with crop cover by equation 9, using an assumed  $Z_o$  of 1.0 centimeter in the wind-function term (10). Improvement in the period totals for each of the 3 days can be observed in table 4, column 4. While the change in  $Z_o$  from 2 centimeters to 1 for June 26 resulted in a slight improvement, the reduction in  $Z_o$  from 20 centimeters to 1 on August 26 resulted in an  $E_p$  estimate that is within 5 percent of the lysimeter value, as compared with a previous overestimate of 100 percent. These results agree favorably with those of Jensen (9), who reported that for a variety of crops in southern Idaho,  $Z_o$  in equation 10 should be approximately 0.75 centimeter where crops were higher than 50 centimeters.

For comparison, the combination equation 9 using Penman's original aerodynamic term (17) was computed hourly and summed to give a total for each day. The results are shown in table 4 column 5. They indicate that the wind function as originally used by Penman produces essentially the same results as the log profile version (10) using a  $Z_o$  value of 1 centimeter.

## DISCUSSION

Most of the meaningful verifications of the Bowen ratio energy budget technique have been reported for low-growing irrigated crops with generally flat topography and uniform fetch conditions. The success of the hourly values of  $E$  computed by equation 3 for the lysimeter at Coshocton, Ohio, tends to verify the application of the approach to estimating evapotranspiration under natural field conditions where fetch and surface homogeneity are less than ideal. The method is capable of predicting actual evaporation from a bare, dry soil with limiting moisture, as well as from a tall crop such as corn (height = 240 centimeters) under a wide range of growth and moisture conditions.

Overcast skies (low direct solar radiation) or variable weather conditions do not appear to limit the application of this technique except, perhaps, during periods of rain. The Bowen ratio method fails during early morning and late evening as a result of increasing relative errors in measuring temperature and humidity profiles during nondaylight hours. However, since  $E$  rates are quite small and are often zero at such times, this failure is relatively unimportant.

Use of average hourly values of  $\Delta T$  and  $\Delta e$ , as measured by the Lourence and Pruitt psychrometer system (14), appears sufficient to give accurate estimates of  $B$  for the Bowen ratio technique. The success of the Bowen ratio method for the estimation of hourly  $E$  flux rates indicates that the micrometeorological measurements of radiation, temperature, and humidity are representative of conditions prevailing at the test site.

The success of the Bowen ratio methods under poor fetch and sometimes variable conditions indicates that fetch requirements are less stringent for this approach as compared with the aerodynamic methods. To give accurate results, the required height of the sensor-to-fetch-distance ratio appears to be no greater than 1 to 50 and possibly smaller. On two occasions, one over corn and the other over bare soil, a height-fetch ratio of about 1 to 10 was adequate. However, on October 16, with wind speeds greater than 500 centimeters per second, a ratio of 1 to 75 was inadequate at one site, whereas the other sampling site with a ratio of 1 to 150 provided an excellent fit with evaporation measured by the lysimeter. Perhaps, during this last sampling period a greater

sampling frequency and a shorter computational period would have improved the estimate of  $E$  by equation 3

On the basis of results with aerodynamic estimates of  $E$  fetch distance appeared to be from 75 to 100 meters for light and moderate wind conditions, up to 150 meters or greater for winds in excess of 500 centimeters per second when the upper profile measurement height was 100 centimeters above the crop surface. A diabatic correction function must be applied to the accepted Thornthwaite and Holzman aerodynamic expression (29), equation 4, during nonadiabatic conditions in order to agree closely with lysimeter and Bowen ratio  $E$  rates. The Keys and Davis empirical correction functions appear to be equally satisfactory; however, occasionally a significant difference between the two approaches occurs. No recommendations can be made on the basis of the tests described here as to the advantages of one correction function over the other. Generally, the aerodynamic method gives better estimates of  $E$  than does the Bowen ratio method only during early morning and late evening hours.

The error analysis tends to indicate that much uncertainty in the aerodynamic methods results from error in measuring or in estimating  $D$ . This error is shown to increase in range as both  $D$  and crop height ( $h$ ) increases. Thus, unless  $D$  is carefully determined by accurate wind-profile analysis, the aerodynamic methods may have a large error when applied over tall vegetation. Thus, aerodynamic methods appear to require better conditions.

Estimates of evapotranspiration with the improved versions of the combination equation, using  $Z_0$

values based on wind profile or crop height, are unsatisfactory once crop height exceeds 75 centimeters. A  $\pm 25$  percent uncertainty in  $Z_0$  results in a probable error of  $\pm 20$  percent in  $E$  (August 27), when  $Z_0 = 20$  centimeters as compared with a 5 percent error in  $E$  if  $Z_0$  were assumed to be measured without error. Since the uncertainty in the determination of  $Z_0$  increases with crop height, resulting in a high degree of uncertainty in potential evapotranspiration estimates over tall vegetation, the use of the log-profile wind function should be limited to bare soil and to crops below 75 centimeters on flat terrain.

Empirical methods can be used to fit a usable wind function in the combination equation. If  $Z_0$  in equation 10 is used as a calibration term as suggested by Jensen (9), then  $Z_0$  in this application should be 1.0 centimeter for corn as high as 240 centimeters. This proposition assumes that no resistance to vapor transport within the corn plant occurred and that the potential evapotranspiration concept is valid as defined. The empirical coefficients proposed by Penman for the wind function of the combination equation appear to be generally applicable to a tall crop such as corn in a humid region. Penman's version (17) gives essentially identical results to Van Bavel's version (3), using a  $Z_0$  of 1.0 centimeter.

Two conclusions are possible from the limited results with the combination equations: (1) There is a resistance to water vapor transport within the corn plant despite high soil moisture conditions or (2) the log-profile wind function is unsatisfactory for application in the combination equation where crop height exceeds 75 centimeters on heterogeneous terrain.

## LIST OF SYMBOLS

<i>Symbol</i>	<i>Explanation</i>	<i>Units</i>
B	Bowen ratio, $B = H/E$	1
D	Displacement parameter, $D = d + z_0$	cm
E	Evaporation energy equivalent	$\text{cal cm}^{-2} \text{ s}^{-1}$
$E_p$	Potential evaporation	$\text{cal cm}^{-2} \text{ s}^{-1}$
G	Heat flux into ground	$\text{cal cm}^{-2} \text{ s}^{-1}$
H	Heat flux into air	$\text{cal cm}^{-2} \text{ s}^{-1}$
$K_h$	Eddy diffusivity for heat	$\text{cm}^2 \text{ s}^{-1}$
$K_m$	Eddy diffusivity for momentum	$\text{cm}^2 \text{ s}^{-1}$
$K_v$	Eddy diffusivity for vapor	$\text{cm}^2 \text{ s}^{-1}$
L	Latent heat of vaporization	585 cal/g
P	Atmospheric pressure	mbar
$R_n$	Net radiation flux	$\text{cal cm}^{-2} \text{ s}^{-1}$
$T_z$	Temperature at height (z)	$^{\circ}\text{C}, ^{\circ}\text{K}$
Z	Height above ground surface	cm
$c_p$	Specific heat at constant pressure	$\text{cal gm}^{-1} ^{\circ}\text{C}^{-1}$
d	Zero plane displacement	cm
$e_a$	Actual vapor pressure of air	mbar
$e_s$	Vapor pressure of air at saturation	mbar
$e_z$	Vapor pressure of air at height (z)	mbar
g	Acceleration of gravity	$\text{cm s}^{-2}$
h	Vegetation height	cm
k	Karman's constant	1
ln	Natural logarithm	
$r_a$	Aerodynamic diffusion resistance	$\text{s cm}^{-1}$

## LIST OF SYMBOLS—Continued

<i>Symbol</i>	<i>Explanation</i>	<i>Units</i>
$r_s$	Surface diffusion resistance	$\text{s cm}^{-1}$
$s$	Slope of saturation vapor pressure curve $s = de/dT$	$\text{mbar } \text{C}^{-1}$
$u_z$	Horizontal wind velocity at height (z)	$\text{cm s}^{-1}$
$z_0$	Roughness length	cm
$\delta$	Wet-bulb depression	$^{\circ}\text{C}, \text{ }^{\circ}\text{K}$
$\epsilon$	Ratio molecular weight water vapor to air	1
$\gamma$	Psychrometer constant, $\approx c_p P/L\epsilon$	$\text{mbar } \text{C}^{-1}$
$\rho$	Density of moist air	$\text{g cm}^{-3}$
$\psi$	Stability profile influence function	1
$\Delta$	Increment	
<b>Subscripts</b>		
$z$	Property at height (z) referenced above ground level.	

## LITERATURE CITED

1) Bartholic, J.F., Namken, L.N., and Wiegand, C.L.  
 1970. Combination equations used to calculate evaporation and potential evaporation. U.S. Dept. Agr., Agr. Res. Serv. ARS 41-170, 14 pp.

2) Bowen, I.S.  
 1926. The ratio of heat losses by conduction and by evaporation from any water surface. *Phys. Rev.*, Ser. 2, No. 27: 779-787.

3) Businger, J.A.  
 1956. Some remarks on Penman's equation for evapotranspiration. *Neth. Jour. Agr. Sci.* 4: 77-80.

4) Fogel, C.M.  
 1962. Introduction to engineering computations. 210 pp. International Textbook Co. Scranton, Pa.

5) Fritschen, L.J.  
 1965. Accuracy of evapotranspiration determinations by the Bowen ratio method. *Bul. Internat. Assoc. Sci. Hydrol.* 10(2): 38-48.

6) 1966. Evapotranspiration rates of field crops determined by the Bowen ratio method. *Agron. Jour.* 58: 339-342.

7) Harrold, L.L., and Dreibelbis, F.R.  
 1958. Evaluation of agricultural hydrology by monolith lysimeters, 1944-55. U.S. Dept. Agr. Tech. Bul. 1179, 166 pp.

8) 1967. Evaluation of agricultural hydrology by monolith lysimeters, 1956-62. U.S. Dept. Agr. Tech. Bul. 1367, 123 pp.

9) Jensen, M.E., Wright, J.L., and Pratt, B.J.  
 1971. Estimating soil moisture depletion from climate, crop and soil data. *Amer. Soc. Agr. Engin. Trans.* 14(5): 954-959. September-October.

10) Kohler, M.A., Nordenson, T.J., and Fox, W.E.  
 1955. Evaporation from pans and lakes. U.S. Weather Bur. Res. Paper 38.  
 and Parmele, L.H.

11) 1967. Generalization estimates of free-water evaporation. *Water Resources Res.* 3(4): 997-1006.

12) Lemon, E.  
 1965. Micrometeorology and the physiology of plants in their natural environment. *Plant Physiol.* 4(A): 203-227, Academic Press, N.Y.

(13) \_\_\_\_\_ 1963. The energy balance at the earth's surface. U.S. Dept. Agr., Prod. Res. Rpt. 71. Part 1. Washington, D.C.

(14) Lourence, F.J., and Pruitt, W.O.  
 1969. A psychrometer system for micrometeorology profile determination. *Jour. Appl. Met.* 8(4): 492-498.

(15) Mukammal, E.I., King, K.M., and Cork, H.F.  
 1966. Comparison of aerodynamic and energy budget techniques in estimating evapotranspiration from a corn field. *Arch. für Met., Geophys., und Bioklim.* 14: 384-395.

(16) Panofsky, H.A., Blackadar, A.K., and McVehil, G.E.  
 1960. The diabatic wind profile. *Quart. Jour. Roy. Met. Soc.* 86: 390-398.

(17) Penman, H.L.  
 1948. Natural evaporation from open water, bare soil, and grass. *Roy. Soc. (London) Proc., Ser A-193(1032):* 120-145.

(18) \_\_\_\_\_ 1956. Estimating evaporation. *Amer. Geophys. Union Trans.* 37: 43-50.

(19) Peterson, F.W.  
 1971. Predictions of the momentum exchange coefficient for flow over heterogeneous terrain. *Jour. Appl. Met.* 10(5): 958-961.

(20) Pruitt, W.O., and Lourence, F.  
 1966. Tests of aerodynamic, energy budget, and other evaporation equations over a grass surface. Final Report 1965, Investigations of Energy, Momentum, and Mass Transfer Near the Ground. U.S. Dept. Army Electronics Command, Atmos. Sci. Lab., pp. 37-63.

(21) Rosenberg, N.J.  
 1969. Seasonal patterns in evapotranspiration by irrigated alfalfa in the central Great Plains. *Agron. Jour.* 61(6): 879-886.

(22) Sellers, W.D.  
 1964. Potential evapotranspiration in arid regions. *Jour. Appl. Met.* 3: 98-104.

(23) \_\_\_\_\_ 1965. *Physical climatology.* Univ. of Chicago Press, 272 pp. Chicago.

(24) Slatyer, R.O., and McIlroy, I.C  
1961. Practical microclimatology CSIRO,  
Plant Ind Div, 328 pp. Canberra,  
Australia

(25) Szeicz, G., and Long, I.F.  
1969. Surface resistance of crop canopies.  
Water Resources Res. 5, 622-633.

(26) Tanner, C B  
1968 Evaporation of water from plants and  
soil, in water deficits and plant growth.  
Ed by T.T Kozlowski V. I: 73-106.  
Academic Press. New York.

(27) \_\_\_\_\_ and Pelton, W.L.  
1960 Potential evapotranspiration estimated  
by the approximate energy balance  
method of Penman. Jour Geophys.  
Res. 64: 3391-3413.

(28) Thornthwaite, C W., and Hare, F.K.  
1965 The loss of water to the air. Met  
Monog. 6(28): 163-180.

(29) \_\_\_\_\_ and Holzman, B.  
1942. Measurement of evaporation from land  
and water surfaces U.S. Dept. Agr.  
Tech. Bul. 817, 143 pp.

(30) Udagawa, T.  
1966. Variation of aerodynamic character-  
istics of a barley field with growth. Jour.  
Agr. Met. 22: 7-14.

(31) Van Bavel, C.H.M.  
1966. Potential evaporation: the com-  
bination concept and its experimental  
verification. Water Resources Res. 2(3):  
455-468.

(32) Webb, E.K.  
1965. Aerial microclimate Met. Monog.  
6(28): 27-55.

## APPENDIX A—PROPAGATION OF ERRORS

To determine the nature of error propagation (4), as error analysis is sometimes called in indirect measurement, consider the quantity  $Y$  which is a function of independent variables  $X_1, X_2, \dots, X_n$  ( $Y = f[X_1, X_2, \dots, X_n]$ ). The change in  $Y$  that is due solely to a change in  $X_1$  may be denoted by  $\partial Y / \partial X_1$ , where  $\partial Y / \partial X_1$  is the partial derivative of  $Y$  with respect to  $X_1$  and where  $\partial Y / \partial X_1$  represents the change in  $Y$  per unit change in  $X_1$ , while  $dx_1$  represents the actual small change in  $X_1$ . The total change in  $Y$  that is due to changes in all the variables is denoted by the symbol  $dY_m$ , where:

$$dY_m = \left| \frac{\partial Y}{\partial X_1} dx_1 \right| + \left| \frac{\partial Y}{\partial X_2} dx_2 \right| + \dots + \left| \frac{\partial Y}{\partial X_n} dx_n \right| \quad (1A)$$

Thus, if  $dx_1, dx_2, \dots, dx_n$  represent the uncertainties in the directly measured quantities  $x_1, x_2, \dots, x_n$ , respectively, and if all the uncertainties are considered additive, then  $dY_m$  represents the maximum uncertainty in  $Y$ . This uncertainty in  $Y$  may be expressed in terms of any desired measure of dispersion, as long as the same measure of dispersion is used for the uncertainties in the directly measured quantities also. However, it is extremely unlikely that the actual error in a calculated quantity will equal the maximum uncertainty expressed by equation 1A.

The uncertainty or possible error in a calculated quantity is represented better by a probable value than by a maximum value. The probable uncertainty ( $dY_p$ ) or error (4) in a calculated quantity ( $Y$ ) is determined by the square root of the sum of the squares of the individual terms in relationship to the maximum uncertainty. The resulting equation is:

$$dY_p = \left[ \left( \frac{\partial Y}{\partial X_1} \right)^2 dx_1^2 + \left( \frac{\partial Y}{\partial X_2} \right)^2 dx_2^2 + \dots + \left( \frac{\partial Y}{\partial X_n} \right)^2 dx_n^2 \right]^{1/2} \quad (2A)$$

Thus, the probable uncertainty or error in  $Y$  depends not only on the uncertainty of each directly

measured quantity but also on the partial derivatives of the equation that represents  $Y$ . A variable would not contribute toward the probable error in  $Y$ , regardless of the value of  $\partial Y / \partial x_1$ , if the uncertainty ( $dx_1$ ) for that variable were zero. The nature of the equation does not contribute directly to the error but rather modifies the errors already present in the measured values.

The following example details the procedure used to evaluate the probable and the maximum error in the Bowen ratio estimate (equation 3) of  $E$ :

By taking the partial derivatives of equation 3 successively with respect to  $R_n$ ,  $G$ ,  $\Delta T$ , and  $\Delta e$ , and by substituting the resulting expressions in 1A and 2A, one can obtain the probable error:

$$dE_p = \sqrt{\left( \left( \frac{1}{1+B} \right)^2 dR_n^2 \right) + \left( \left( \frac{1}{1+B} \right)^2 dG^2 \right) + \left( \left[ \frac{(-R_0 + G)}{(1+B)^2} \frac{B}{\Delta T} \right]^2 d\Delta T^2 \right) + \left( \left[ \frac{(R_n + G)}{(1+B)^2} \frac{B}{\Delta e} \right]^2 d\Delta e^2 \right)} \quad (3A)$$

and for the maximum uncertainty

$$dE_n = \left| \left( \frac{1}{1+B} \right) dR_n \right| + \left| \left( \frac{1}{1+B} \right) dG \right| + \left| \frac{(-R_0 + G)}{(1+B)^2} \frac{B}{\Delta T} d\Delta T \right| + \left| \frac{(R_n + G)}{(1+B)^2} \frac{B}{\Delta e} d\Delta e \right| \quad (4A)$$

where  $dR_n$ ,  $dG$ ,  $d\Delta T$ , and  $d$  represent the probable error in measurement of the variables  $R_n$ ,  $G$ ,  $\Delta e$ , respectively.

On May 2, between 1300 and 1400, the following values were observed:

$$\begin{aligned} R_n &= 0.620 \text{ cal/cm}^2 \cdot \text{min.} \\ G &= -0.055 \text{ cal/cm}^2 \cdot \text{min.} \\ \Delta T_{10-100.} &= 3.77^\circ \text{C} \\ \Delta e_{10-100.} &= 1.507 \text{ mbar} \\ E &= 0.221 \text{ cal/cm}^2 \cdot \text{min.} \end{aligned}$$

The value of the probable measurement error for each variable was derived from table 2. By substituting this error in equations 3A and 4A, one derives the following error estimates.

$$\begin{aligned} dE_p &= \pm 0.012 \text{ cal/cm}^2 \cdot \text{min.} \\ dE_m &= \pm 0.018 \text{ cal/cm}^2 \cdot \text{min.} \end{aligned}$$

Thus,  $E \text{ at } 1400 = 0.221 \pm 0.012 \text{ cal/cm}^2 \cdot \text{min.}$  Equations similar to 3A and 4A were developed from equations 8 and 9 by the procedure outlined above for error analysis of these estimates.

### Aerodynamic Equation

$$E = \frac{\epsilon \lambda \rho k^2 \Delta e \Delta u}{[\ln(Z_2 - D/Z_1 - D)]^2} \quad (5A)$$

Letting  $A = \epsilon \lambda \rho k^2$  and assuming that  $Z$  is measured without error, the probable error in estimate of  $E$  is:

$$\begin{aligned} dE_p &= \sqrt{\left[ \left[ \frac{A \Delta u}{\ln(Z_2 - D/Z_1 - D)} \right]^2 d\Delta e^2 + \right.} \\ &\quad \left. \left[ \left[ \frac{A \Delta e}{\ln(Z_2 - D/Z_1 - D)} \right]^2 d\Delta u^2 \right] + \right. \\ &\quad \left. \left[ \left[ \frac{2A \Delta e \Delta u (Z_2 - Z_1)}{\ln(Z_2 - D) (Z_1 - D) (Z_2 - D)} \right]^2 dD^2 \right] \right] \quad (6A) \end{aligned}$$

The maximum uncertainty of  $E$  is:

$$\begin{aligned} dE_m &= \pm \left[ \left[ \left( \ln \left[ \frac{Z_2 - D}{Z_1 - D} \right] \right)^2 d\Delta e \right] + \right. \\ &\quad \left. \left[ \left[ \frac{A \Delta e}{\ln(Z_2 - D/Z_1 - D)} \right]^2 d\Delta u \right] + \right. \\ &\quad \left. \left[ \left[ \frac{2A \Delta e \Delta u (Z_2 - Z_1)}{\ln(Z_2 - D) (Z_1 - D) (Z_2 - D)} \right]^2 dD \right] \right] \quad (7A) \end{aligned}$$

### Stability Correction

$$\psi = \left[ 1 - \frac{bg \Delta T \Delta Z}{T_{abs} (\Delta u)^2} \right]^{-1/4} \quad (8A)$$

The probable error ( $d\psi_p$ ) for the estimate of  $\psi$  is:

$$\begin{aligned} d\psi_p &= \pm \sqrt{\left[ \frac{bg \Delta Z}{4 \psi^5 T_{abs} (\Delta u)^2} \right]^2 d\Delta T^2 +} \\ &\quad \left[ \frac{bg \Delta T}{4 \psi^5 T_{abs} (\Delta u)^2} \right]^2 d\Delta Z^2 + \\ &\quad \left[ \frac{-bg \Delta T \Delta Z}{4 \psi^5 (T_{abs})^2 (\Delta u)^2} \right]^2 dT_{abs}^2 + \\ &\quad \left[ \frac{-bg \Delta T \Delta Z}{2 \psi^5 (T_{abs}) (\Delta u)^3} \right]^2 d\Delta u^2 \quad (9A) \end{aligned}$$

The maximum uncertainty of  $\psi$  is:

$$d\psi_m = \pm \frac{bg}{4\psi^5} \left\{ \left| \left( \frac{\Delta Z}{T_{abs} \Delta u^2} \right) dT \right| + \left| \left( \frac{T}{T_{abs} \Delta u^2} \right) d\Delta Z \right| + \left| \left( \frac{\Delta T \Delta Z}{(T_{abs})^2 (\Delta u)^2} \right) dT_{abs} \right| + \left| \left( \frac{-2\Delta T \Delta Z}{T_{abs} (\Delta u)^3} \right) d\Delta u \right| \right\} \quad (10A)$$

The maximum uncertainty of  $E_p$  is:

$$d(E_p)_m = \frac{S}{S+\gamma} \left| dR_b \right| + \left| dG \right| +$$

### Combination Equation for Potential ET

$$E_p = \frac{S}{S+\gamma} \left[ (R_n + G) + \frac{\rho C_p k}{LS} \frac{u(e_s - e_a)}{\ln\left(\frac{Z-D}{z_o}\right)} \right]^2 \quad (11A)$$

Assuming that  $S$  can be calculated without error, the probable error in estimate of  $(E_p)$  is:

$$d(E_p)_p = \frac{S}{S+\gamma} \sqrt{dR_n^2 + dG^2 + \left[ \frac{\rho C_p K^2 (e_s - e_a)}{LS} \left[ \ln\left(\frac{Z-D}{z_o}\right)^{-2} \right] 2du^2 + \left[ \frac{\rho C_p K^2 u}{LS} \left[ \ln\left(\frac{Z-D}{z_o}\right)^{-2} \right]^2 d(e_s - e_a)^2 \right] + \frac{2\rho C_p K^2 (e_s - e_a) u}{LS \ln\left(\frac{Z-D}{z_o}\right)^2 3(Z-D)^2} dD^2 \right] + }$$

$$\left| \left[ \frac{\rho C_p k (e_s - e_a)}{LS \left[ \ln\left(\frac{Z-D}{z_o}\right)^2 \right]} \right] du \right| +$$

$$\left| \left[ \frac{\rho C_p K^2 u}{LS \left[ \ln\left(\frac{Z-D}{z_o}\right)^2 \right]} d(e_s - e_a) \right] + \right|$$

$$+ \left| \left[ \frac{2\rho C_p K (e_s - e_a) u}{LS \left[ \ln\left(\frac{Z-D}{z_o}\right)^3 (Z-D) \right]} dD \right] + \right|$$

$$+ \left| \left[ \frac{2\rho C_p K^2 (e_s - e_a) u}{LS \left[ \ln\left(\frac{Z-D}{z_o}\right)^3 z_o \right]} dz_o \right] \right|$$

(13A)

## APPENDIX B—INSTRUMENTATION AND DATA REDUCTION

### Lysimeter

The weighing lysimeter that was used to measure  $E$  directly has already been described in detail (7, 8). The wide concrete perimeter between the lysimeter and the surrounding field, as originally constructed, has since been removed, and crop planting has been brought to the very edge of the lysimeter. The automatic weighing mechanism records weight changes in the 59,000 kilogram mass to a 2.26-kilogram accuracy, which is equivalent to approximately 0.25 millimeter of water over the lysimeter surface area. Average hourly  $E$  was obtained by averaging the six consecutive 10-minute weights beginning at 60 minutes before each hour and ending at the hour. This averaging process in weight records removed wind-caused irregularities.

### Wind Profile Measurement and Data Reduction

The wind profile measurements at the lysimeter site were made with four matched rotating cup anemometers that had been manufactured by Wong Laboratories. These were mounted 50, 100, 150, and 200 centimeters above the crop surface. The sensors produced electrical contact closure for every 0.1 mile of wind passage, sending an impulse to a Sodeco printing counter. The total number of impulses for each hour was printed on the hour, providing the average wind speed in miles per hour.

Wind-profile measurements at the central watershed site were made during three of the seven runs. During the July 24 run, a system of six Thornthwaite rotating-cup anemometers was used. Impulses were counted on mechanical counters. These anemometers produce an impulse for approximately every 1.5 meters of wind movement. During the runs of October 14 and 16, a Beckman and Whitley system of three rotating-cup anemometers was used. Impulses were counted on mechanical counters that were photographed on microfilm every 15 minutes. These anemometers produced an impulse for approximately every 1.5 meters of wind movement. The total number of counts for each hour was recorded and converted to average wind speed in centimeters per second.

The methods used to evaluate  $D$  and  $z_0$  were subject to shortcomings and required sensitive instrumentation, suitable fetch, and neutral

atmospheric conditions. Temperature gradients and elastic properties of vegetation combined to make  $D$  and  $z_0$  difficult to characterize for vegetated surfaces. Since temperature gradients are relatively small over vegetation, plant geometric properties are the greatest influence on  $D$  and  $Z_0$ . Therefore, the parameters can be expressed as a function of crop height as shown in figure 9 (12).

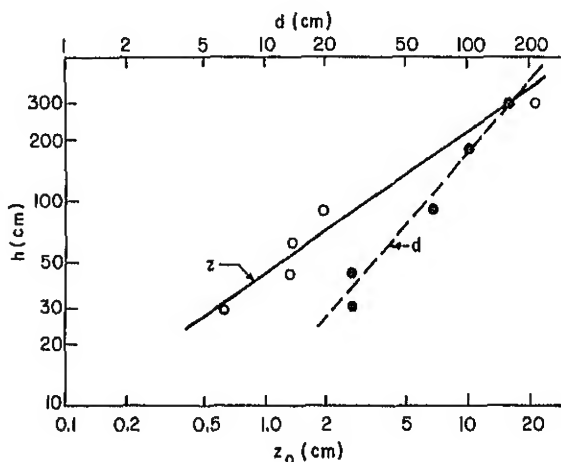


Figure 9.—Roughness length ( $z_0$ ) and zero plane displacement ( $D$ ) as a function of height of the corn crop ( $h$ ) during the 1961 growing season at Ellis Hollow, N.Y. (12). Values are for near-isothermal conditions and wind speeds of 100 to 400 cm/s at the 1-meter level above the crop surface

Wind-profile parameters were determined by graphical data where  $\ln(Z-D)$  is visually plotted against wind speed and forced through intercept  $Z_0$  values. Since the data points were often too scattered to provide a precise determination of  $Z_0$  and  $D$ , these values were first estimated on the basis of wind-profile parameters measured over corn of equal height ( $h$ ) at Ithaca, N.Y. (figure 9). This transformation is possible because of the similarity in "Leaf Area Index" (LAI) between the corn at Ellis Hollow, N.Y., and the corn used in this study (table 5). Except for 1 day (October 14), the transposed  $D$  and  $Z_0$  values provided a good fit to match the hourly wind-profile data. On October 14, the  $D$  and  $Z_0$  that gave the best straight line fit between  $\ln(Z-D)$  and wind speed were chosen. Values of  $u_2$  and  $u_1$  were taken from the straight line plot for each hour of heights ( $Z_2 - D$ ) and ( $Z_1 - D$ ) for use in appropriate equations.

Table 5.—A comparison of leaf area index (LAI) at Ellis Hollow, N.Y., and Coshocton, Ohio, locations as a function of relative height (Z/h)

Z	Z/h	$\Sigma$ LAI Ellis Hollow <sup>1</sup>	$\Sigma$ LAI Coshocton <sup>1</sup>
240	1.00	0	0
227	.95	.08	.08
189	.78	.40	.40
135	.56	1.90	1.90
81	.34	3.20	3.20
37	.15	4.00	3.60
0	0	( <sup>2</sup> )	( <sup>3</sup> )

<sup>1</sup> Accumulated LAI from top of crop downward

<sup>2</sup> Base level of Ellis Hollow, N.Y., corn crop = 4.5 LAI.

<sup>3</sup> Base level of Coshocton, Ohio, corn crop; LAI not known

### Wet- and Dry-Bulb Air Temperature Instrumentation

An aspirated psychrometer system modeled after a system developed and tested at Davis, Calif., (14) was used to measure temperature and humidity profiles. The wet-bulb air temperature measurement and the water supply were redesigned from the Davis system. Changes were also made in the mast and clamping system, and minor modifications were made in the sensor-holding assembly. Two separate profile systems were used: (1) A 10-level profile system in midwatershed site and (2) a 5-level profile system at the lysimeter site. In the five level profile system, all measurements were taken above the crop canopy. The psychrometer systems provided measurements of temperature and humidity accurate to  $\pm 0.020^\circ\text{C}$  and  $\pm 0.10$  millibar, respectively.

Figure 10 presents a cutaway diagram of a dry- and wet-bulb assembly. The dry-bulb thermopile wires are encased within a thin-walled, stainless-steel tube, five-sixteenths of an inch in diameter. These wires emerge from the upwind and extend 4 centimeters beyond the end of the tube. Because the cool wet-bulb element lies parallel to this tube for some distance, some cooling effects can result. Having a tube of low thermal conductivity minimizes the rate at which heat can be conducted along this tube from the region where the dry-bulb thermopiles are located. A rubber sleeve shrouds the dry-bulb thermopile elements that extend from the stainless-steel tube. This rubber sleeve also fits snugly over the end of the stainless-steel encasement tube. The wires are encapsulated within this sleeve with silicone rubber.

The dry-bulb sensor consists of a five-junction thermopile set referenced to the dry-bulb element of

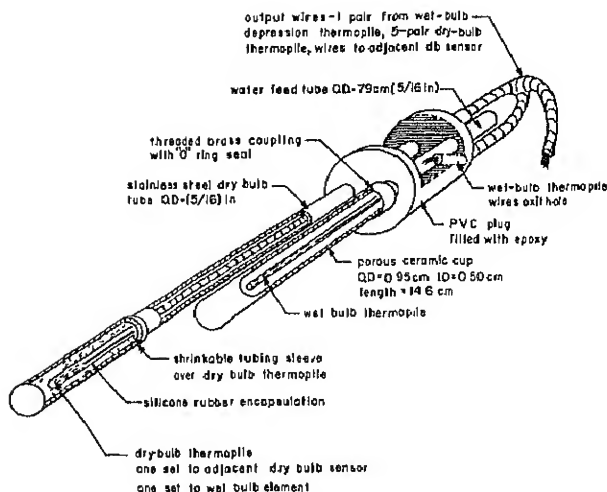


Figure 10.—Cutaway view of wet-bulb and dry-bulb assembly used in psychrometer system

other sensors. An additional independent five-junction thermopile set extends back through the mounting plug and into the wet-bulb element contained on the same sensor plug assembly. The dry-bulb temperature differential system shown in figure 11 permitted a more precise measurement of the dry-bulb temperature profile and use of the recording system already on hand. At the lower level

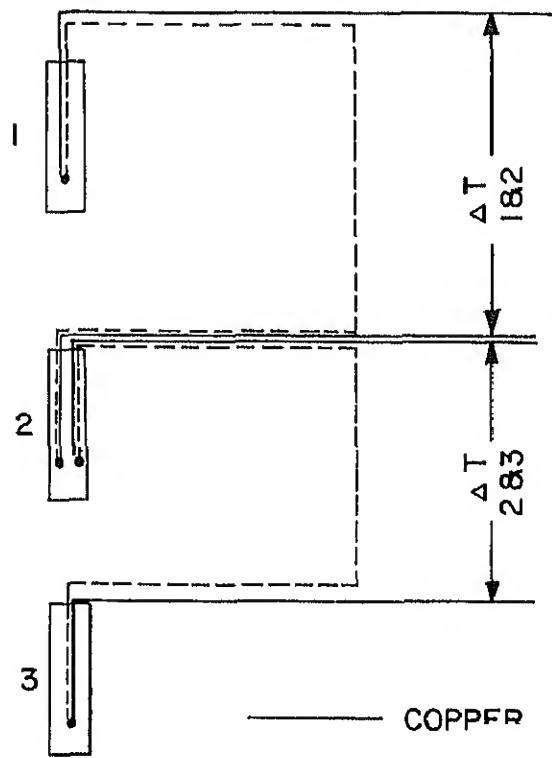


Figure 11.—Dry-bulb thermopile profile

sensor, dry-bulb temperature was referenced to an ice bath located at the base of the mast, or the dry-bulb temperature was referenced to ice with a small thermocouple that had been encased along with the dry-bulb thermopile.

The wet-bulb element, which is shown in figure 12, is not a conventional cotton-wick type, but a porous ceramic cup 14.6 centimeters long.

Water is supplied to the porous cup through a clear plastic tube that leads from a supply bottle located on the main sensor-mounting arm. This tube is connected to a 0.79-centimeter (five-sixteenth of an

inch) diameter stainless-steel tube that passes through the sensor assembly mounting plug. The porous wet-bulb element is attached to this stainless-steel tube with a threaded-brass connector.

One advantage of the ceramic-cup, wet-bulb element is a closed water system. This system eliminates part of the problem associated with the wet cotton-wick system, where a free water surface was required to supply moisture for evaporation on the wick. The ceramic wick does not flood when the elevated waterhead is subject to evaporation, and when the waterhead is slightly negative, water still

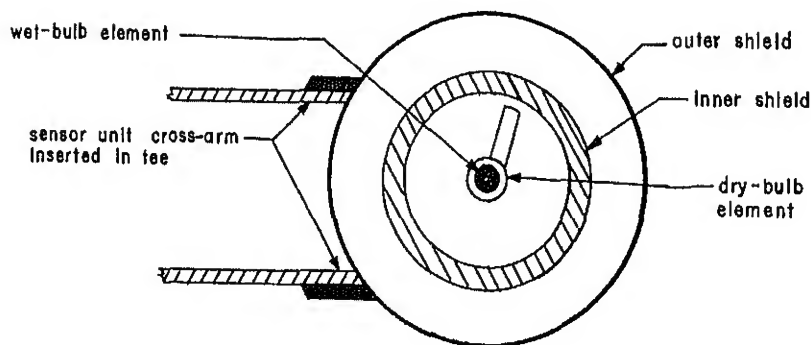
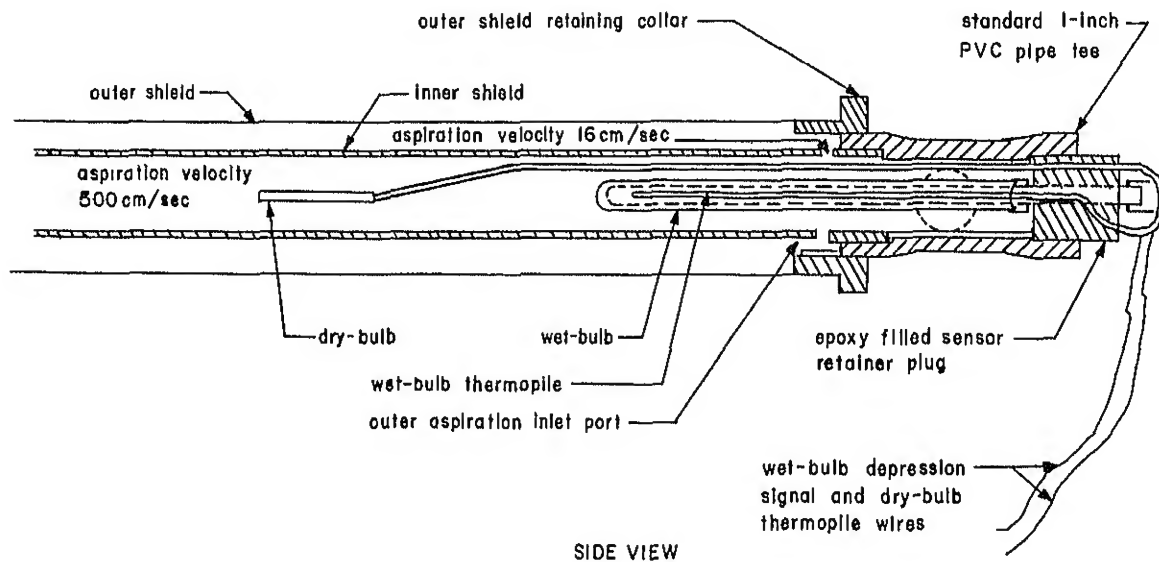


Figure 12.—Details of sensor unit and aspirated shield used on psychrometer system.

continues to move into the ceramic element because the element acts as a tensiometer with a continuous water column. However, one must bleed all the entrapped air in the wet-bulb water system before starting to operate. Under most field conditions, the water bottle reservoir does not require refilling more often than every 24 hours.

The wet-bulb thermopile wires run inside the porous ceramic cup to a point near the forward end where the sensing junctions are located. These wires leave the water-filled media through a hole drilled at an angle from the back of the epoxy mounting plug and through the side of the 0.79-centimeter (five-sixteenth of an inch) diameter, stainless-steel, water-feed tube. This exit hole is later sealed by refilling with epoxy after the sensor wires are properly positioned. The five thermopile wires extend into the dry-bulb tube that has been described earlier. The two wet-bulb thermopile output lead wires originate from the wet-bulb end and pass from the sensing plug with the thermopiles and follow the dry-bulb thermopile wires that lead directly to the recording system.

Figure 12 shows a scale drawing of a sensor unit and its radiation shielding tubes. A double shield arrangement that has been patterned after the Davis design is used. The outer shield consists of an epoxy fiberglass tube 0.12 centimeter (0.047 inch) thick, while the inner tube is a standard 1-inch-type 1 PVC pipe. The outer surfaces of each shield are covered with a layer of adhesive mylar-coated aluminum foil.

Air is drawn past the dry- and wet-bulb sensors at a velocity of 500 centimeters per second. A small 115-VAC fan capable of moving 15 cubic feet of air per minute while requiring 7 watts of power does this. Air is also drawn between the inner and outer shields at a rate of 16 centimeters per second through six small bleed holes located on the back end of the inner shield tube. This aspiration insures removal of any heat loading caused by radiative or conductive sources. Figure 13 shows complete dry- and wet-bulb unit along with all of its disassembled components.

A test was performed to determine the time-response characteristics of the dry- and wet-bulb elements in order to achieve good phase relationship between the wet-bulb and the dry-bulb temperature responses when the units were subjected to abrupt changes in temperature. A time constant of 20 to 25 seconds after an abrupt change of  $7.5^{\circ}\text{C}$  was necessary to achieve 62 percent of the final temperature. During construction, each thermopile junction was checked for proper insulation and for verification that its response at a given temperature was within  $\pm 10$  microvolts of one another. The final

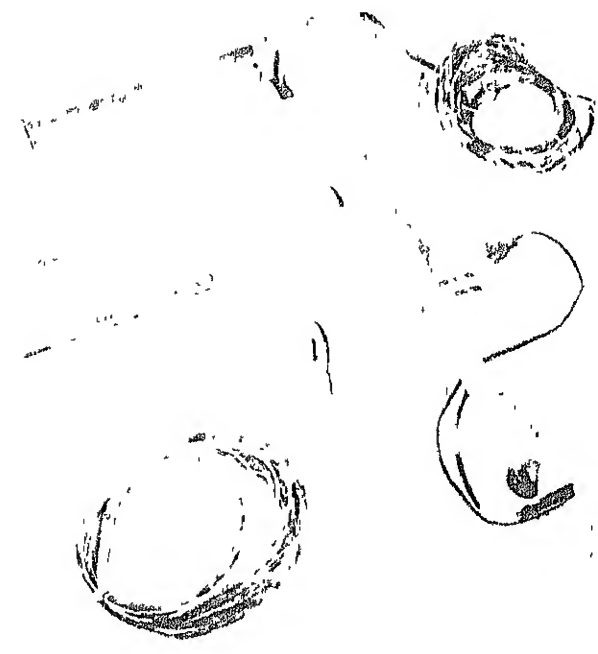


Figure 13.—Complete dry- and wet-bulb unit along with its disassembled components

calibration constant for the 5 junction thermopile assemblies was:

$$^{\circ}\text{C} = 4876^{\circ}\text{C}/\text{mv}$$

Two profile masts were outfitted with the temperature sensors described. Figure 14 shows the level masts with the various sensor spacing used. A Condor steel-channel tower 10 meters long was outfitted with sensor units. The sensor units were mounted with 1-inch clamps. Allen wrench set screws permitted adjustment of the sensor units in a vertical direction. The dry-bulb reference thermopile sets extended about 2 meters from the mast's base, which had been placed in an ice reference bath contained in a large, foam-plastic ice pail.

The differential millivolt signals for temperature difference and wet-bulb depression were recorded on a multichannel millivolt recorder (L & N Speedomax Type G). A summary of these measurements is contained in table 6. The recorder was connected by shielded-copper leads to the differential thermopile system.

Instantaneous microvolt readings of temperature difference and wet-bulb depression were taken from the strip chart records at 5-minute intervals and

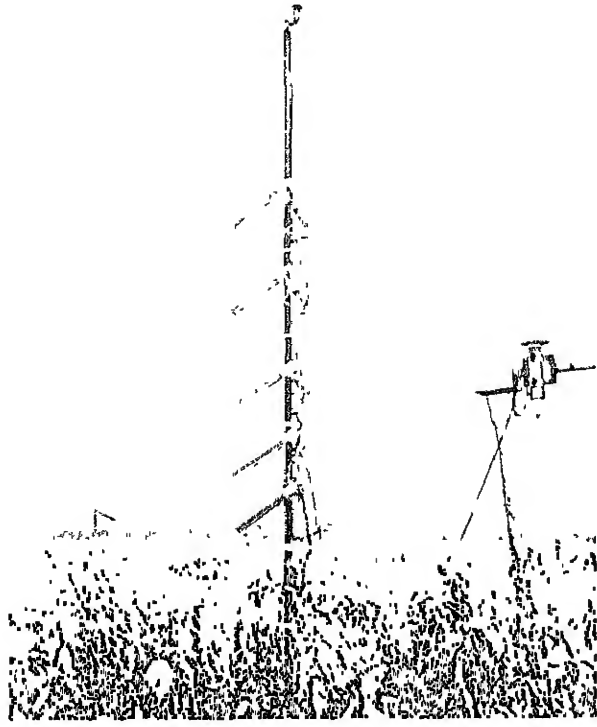


Figure 14—Complete five-level, dry- and wet-bulb temperature mast.

averaged on an hourly basis. These data were then converted from microvolts to degrees Celsius, and average hourly dry-bulb and wet-bulb depression temperatures were computed. By knowing the dry-bulb temperature and wet-bulb depression at each sampling level, computing vapor pressure of the air for each hour period was then possible.

The dry-bulb air temperature ( $^{\circ}\text{C}$ ) and vapor pressure ( $\text{g}/\text{m}^3$ ) were plotted against the  $\ln (Z-D)$ , where  $D$  was determined from wind-profile analysis. A straight line was drawn visually to provide the best fit for the data points for a given hour. Values of  $e_2$ ,  $e_1$ ,  $T_2$ , and  $T_1$  were taken from the straight line plot for each hour at heights  $(z_2 - D)$  and  $(z_1 - D)$  for use in the required computations.

#### Description of Other Temperature Measurements and Data Reduction

Other temperature measurements made at lysimeter Y102C are summarized in table 6. Briefly, all absolute temperature data were recorded on a 16-channel Leeds and Northrup speedomax G thermocouple recorder with a range of  $-20^{\circ}$  to  $120^{\circ}$  F and a sensitivity of  $0.25^{\circ}$  F. Dry-bulb and wet-bulb

temperature measurements were made in each of the five aspirated sensor assemblies described in the temperature and humidity profile section. These measurements provided an absolute temperature measurement for the thermopile psychrometric system and served as a check in comparison with absolute temperature computed for each profile level.

Instantaneous temperature data were taken from the strip chart records at 10-minute intervals and tabulated for each 24-hour period. All readings were converted from degrees Fahrenheit to degrees Celsius and average hourly values were computed from the 10-minute values.

Soil surface temperature was measured by the Barnes IT3 infrared thermometer. The infrared thermometer instrument calibration was obtained by observing the millivolt output of the thermometer sensor while reading a black-body surface of known temperature. The complete curve for the working range of the instrument was determined by repeating the procedure at various temperatures in a water bath calibration source that duplicated black-body conditions. The output signal from the IT3 console was recorded on a Royson electronic integrator that had an accuracy of  $\pm 0.1^{\circ}$  C. for the complete system. The millivolt output from the Barnes infrared thermometer was averaged for each hour, and the equivalent temperature in  $^{\circ}\text{C}$  was determined from the calibration curve of temperature versus millivolt output.

#### Description of Radiation Measurement and Data Reduction

A summary of the radiation measurements made at lysimeter Y102C is given in table 7. All the sensors were purchased commercially, except for the miniature net radiometers, which were fabricated at the Water Conservation Laboratory at Phoenix, Ariz. The manufacturer's calibration had to be accepted for each instrument since no source of calibration was available. However, by comparing the output from similar sensors exposed during a period of steady solar radiation, a field calibration can be achieved.

All the radiation sensors were located at sites that were mostly free from any obstructions above the plane of the sensing element. Fritsch net radiometers Nos. 432 and 567 and the inverted Eppley No. 7583D1 were all mounted on the end of a 2-meter boom that was pivoted from a 4-inch diameter mast 4 meters high. The mast was located on the north side of the lysimeter with the boom containing the sensors extending to the south over the

Table 6.—A summary of temperature and wind measurements made at Coshocton, Ohio, summer 1969

Observation	Sensor	Value recorded	Recording system	Sensitivity of recording system	Height of sensor	Location
Air temperature (shielded and ventilated).	Thermopile	Instantaneous mV output at 5-min intervals converted to temperature °C (av. for hour)	L & N speedomax G, mV strip chart recorder.	0.005° C	5 levels above crop surface. Some specific sensor levels given on daily profile data of (C), (G/m <sup>3</sup> ), (cm/s).	Lysimeter Y102C.
Wet-bulb temperature (shielded and ventilated)	-- do --	-- do --	-- do --	0.010° C	-- do -- (10 levels in all).	-- Do -- Watershed WS 101 site center.
Air temperature (shielded and ventilated)	-- do --	Instantaneous temperature at end of each 10-min period (av. for hour).	L & N speedomax G temperature strip chart recorder.	0.25° F	5 levels above crop surface.	Lysimeter Y102C.
Wet-bulb temperature (shielded and ventilated).	Thermocouple with ceramic wick.	-- do --	-- do --	0.25° F	-- do --	-- Do --
Soil temperature.	Thermocouple.	-- do --	-- do --	0.25° F	0.05 m below ground surface.	-- Do --
Soil surface temperature.	Barnes infrared thermometer, IT-3, #493.	Integrated hourly av. temperature	Roxson electronic integrator.	0.1° C	1.0 m above soil surface.	-- Do --
Wind	1 Wong cup anemometer	Av wind speed for each hour.	Sodeco printing counter.	1 count for each 0.1-mi wind.	2.4, 2.6, 3.0, and 2.0 m above crop surface.	Watershed WS 101 (all runs).
	2 Thorn-thwaites cup anemometers.	-- do --	Mechanical counters (visual reading).	1 count for each 1.5-m wind	2.4, 2.6, 3.0, 3.8, 4.6, 5.4 m h = 2.4 m.	Watershed WS 101 (7/24/69).
	3 Beckman and Whittley cup anemometers.	-- do --	Mechanical counters (microfilm recording @ 15 min.	-- do --	1.8, 2.3, 3.3 m (10/14) h = 1.3 m. 0.5, 1.1, 1.6 m (10/16) h = 0 cm.	Watershed WS 101 (10/14), (10/16).
Wind direction.	Beckman and Whittley vane.	Compass point av. for hour.	Strip chart recorder.	±10°	10 m above soil.	Lysimeter Y102C.

Table 7.—A summary of radiation measurements made at Coshocton, Ohio, summer 1969

Observation	Sensor and serial no.	Calibration constant	Value recorded	Recording system	Sensitivity of recording system	Height of sensor	Location
		<i>Mv/langley</i>			<i>Langley/min</i>		<i>M</i>
Net radiation.	1 Fritschen miniature net #432.	3.12	Integrated hourly from continuous measurement.	Royson electronic integrator.	0.005	1 above crop surface.	Lysimeter Y102C.
	2 Fritschen miniature net #567.	3.42	-- do --	-- do --	.0005	-- do --	-- do --
	3 Fritschen miniature net #548.	3.43	-- do --	-- do --	.0005	-- do --	Center of treated watershed WS 101.
Incoming total hemispherical radiation.	Beckman & Whitley total ventilated.	1.27	-- do --	-- do --	.001	-- do --	Lysimeter Y102C.
Soil heat flux.	Beckman & Whitley soil heat flux plates #540, #541.	7.7	-- do --	-- do --	.00015	0.05 below soil surface.	-- do --
Incoming solar radiation.	Eppley 180° temperature compensated #7734.	5.70	Continuous trace and integrated hourly.	L & N speedo- max H and integrator.	.0015	4 above crop surface.	-- do --
Reflected solar radiation.	Eppley precision model 2 #758301 (inverted).	5.35	-- do --	L & N speedo- max H and disc integrator.	.0015	1 above crop surface.	-- do --

lysimeter. Thus, the sensors were completely free of obstructions except for the mast, which, for practical purposes being to the north of the sensors, had no influence.

Many radiation sensors were connected directly to electronic integrators. Each integrator system consisted of a Royson lectro-count which converted the incoming millivolt signal to a pulse rate, the pulse rate being directly proportional to the magnitude of the input signal. This pulse output from the electronic integrator was then totalized on Sodeco printing counters. The Sodeco units were programmed to print the total counts for each hour on a paper tape and to

reset to zero after printout. Thus, the integrated value of radiation from a sensor could be obtained by multiplying the count output for each hour by the integrator calibration constant and then by the sensor calibration constant.

Two Leeds and Northrup Speedomax H strip chart recorders were equipped with disc integrators and General Electric printing demand meters. These units had been assembled by Eppley laboratories for use with their Eppley pyranometers. The output from the printing demand meter gave the total value of integrated radiation for each half-hour period in langleys.

## APPENDIX C—AVERAGE HOURLY PROFILE DATA

This appendix lists average hourly profile data for each day on which observations were made. Data are presented in the following order:

1. Average hourly lysimeter evaporation and

energy balance components at lysimeter and midwatershed sites.

2. Smoothed profile data from log-linear plots of temperature, humidity, and wind at lysimeter and midwatershed sites.

## AVERAGE HOURLY LYSIMETER EVAPORATION, RADIATION, AND SOIL HEAT FLUX RATES

LYSIMETER SITE Y102-C, COSHOCON, WISCONSIN

DATE - 5/ 21/ 69

TIME OF PERIOD	END LE(1)	ENERGY BALANCE - CAL/CM <sup>2</sup> -MIN	RADIATION COMPONENTS - CAL/CM <sup>2</sup> -MIN				
			H(2)	G(3)	RN(4)	QS(5)	RQS(6)
5	0.000	0.130	0.020	-0.150	0.000	0.000	0.000
6	0.000	0.128	0.013	-0.141	0.000	0.000	0.000
7	0.000	0.092	0.008	-0.100	0.159	0.040	0.000
8	-0.056	-0.009	-0.006	0.071	0.412	0.091	0.000
9	-0.112	-0.108	-0.026	0.246	0.688	0.142	0.000
10	-0.223	-0.133	-0.046	0.402	0.941	0.135	0.000
11	-0.167	-0.329	-0.055	0.551	1.146	0.213	0.000
12	-0.167	-0.406	-0.055	0.632	1.251	0.231	0.000
13	-0.167	-0.446	-0.056	0.669	1.275	0.235	0.000
14	-0.223	-0.342	-0.055	0.620	1.195	0.221	0.000
15	-0.112	-0.391	-0.046	0.545	1.062	0.137	0.000
16	-0.112	-0.266	-0.040	0.418	0.830	0.163	0.000
17	-0.056	-0.158	-0.036	0.250	0.651	0.116	0.000
18	0.000	-0.028	-0.015	0.043	0.365	0.057	0.000
19	0.000	0.097	0.013	-0.110	0.128	0.020	0.000
20	0.000	0.147	0.001	-0.148	0.005	0.006	0.000
21	0.000	0.149	0.001	-0.150	0.000	0.000	0.000
22	0.000	0.147	0.001	-0.148	0.000	0.000	0.000

(1) LE FROM LYSIMETER, (-) SIGN INDICATES FLUX AWAY FROM SURFACE

(2) SENSIBLE HEAT FLUX, H = - (LE + G + RN), (3) G = SENSIBLE HEAT FLUX

(4) RN = NET RADIATION, (5) RS = INCOMING GLOBAL SOLAR RADIATION

(6) QS = REFLECTED GLOBAL SOLAR, (7) QAT = INCOMING ALL WAVE RADIATION

AVERAGE\_HOURLY\_LYSIMETER\_EVAPORATION,\_RADIATION,\_AND\_SOIL\_HEAT\_FLUX\_RATES

LYSIMETER SITE Y102-C CONSTRUCTION UNIT

DATE = 54-221-65

TIME END OF PERIOD	ENERGY BALANCE - CAL/CM2-MIN	RN(4)	RN(3)	RADIATION COMPONENTS - CAL/CM2-MIN	RAT(7)
5	-0.004	3.132	0.018	-0.146	0.000
6	-0.020	2.151	0.017	-0.142	0.020
7	-0.047	0.119	0.035	-0.081	0.095
8	-0.075	0.037	-0.002	0.049	0.273
9	-0.100	0.113	-0.033	-0.010	0.177
10	-0.105	0.132	-0.033	-0.024	0.135
11	0.000	0.066	-0.004	-0.052	0.113
12	-0.050	0.104	-0.031	-0.043	0.120
13	-0.083	-0.045	-0.007	0.135	0.326
14	-0.225	-0.127	-0.016	0.368	0.537
15	-0.345	-0.112	-0.027	0.484	0.307
16	-0.195	-0.135	-0.031	0.361	0.760
17	-0.140	-0.067	-0.021	0.228	0.272
18	-0.100	0.102	-0.026	0.004	0.120
19	-0.042	0.136	-0.090	0.056	0.322
20	-0.019	0.122	-0.011	-0.115	0.013
21	-0.018	0.134	0.012	-0.129	0.000
22	0.000	0.108	0.012	-0.121	0.000

(1) LE FROM LYSIMETER, (-) SIGN INDICATES FLUX AWAY FROM SURFACE

(2) SENSIBLE HEAT FLUX, LE = (LE+GRN), LE+GRN = SOIL HEAT FLUX

(3) RN = NET RADIATION, RN = INCIDING GLOBAL SOLAR RADIATION

(4) RS = REFLECTED GLOBAL SOLAR, RS = INCIDING ALL HAVE RADIATION

## AVERAGE HOURLY LYSIMETER, EVAPORATION, RADIATION, AND SOIL HEAT FLUX RATES

LYSIMETER SITE Y102-C CCSHOOTON, OHIO

DATE - 6/ 26/ 65

TIME OF PERIOD	END LYSIME TER H(1)	ENERGY BALANCE - CAL/CM <sup>2</sup> -MIN	RADIATION		COMPONENTS - CAL/CM <sup>2</sup> -MIN	
			RN(3)	RN(4)	QS(5)	RQS(6)
5	0.000	3.116	C.001	-C.117	0.000	0.000
6	0.000	0.050	0.201	-0.051	0.042	0.003
7	-0.112	0.030	-0.007	C.089	0.212	0.350
8	-0.278	0.021	-0.020	0.277	0.438	0.033
9	-0.278	-0.061	-C.034	C.373	0.585	0.111
10	-0.558	0.032	-0.037	0.563	0.813	0.150
11	-0.725	-0.004	-C.044	0.773	1.120	0.135
12	-0.837	-0.032	-C.039	0.903	1.280	0.198
13	-0.892	0.085	-0.025	C.932	1.155	0.190
14	-0.837	0.005	-C.024	C.856	1.130	0.190
15	-0.837	0.076	-0.022	0.783	1.098	0.138
16	-0.612	-0.066	-0.037	C.716	0.977	0.170
17	-0.502	0.036	-C.035	C.521	0.750	0.137
18	-0.278	0.055	-0.022	C.245	0.420	0.032
19	-0.112	0.066	-0.037	C.053	0.203	0.054
20	-C.112	0.198	-C.001	-0.285	0.238	0.003
21	-0.056	0.193	C.003	-C.1+C	0.006	0.300
22	0.000	0.075	C.302	-0.377	0.000	0.442

(1) LE FROM LYSIMETER. (+) SIGN INDICATES FLUX AWAY FROM SURFACE

(2) SENSIBLE HEAT FLUX,  $L = (L_E + G + R_N)$ , (3)  $G = \text{SOIL HEAT FLUX}$ 

(4) RN = NET RADIATION, (5) QS = INCOMING GLOBAL SOLAR RADIATION

(6) RQS = REFLECTED GLOBAL SOLAR, (7) QAT = INCOMING ALL WAVE RADIATION

## AVERAGE\_HOURLY\_LYSIMETER\_EVAPORATION,\_RADIATION,\_AND\_SOIL\_HEAT\_FLUX\_RATES

LYSIMETER SITE Y102-E  
CSECTION .0H10

DATE = 7/24/69

TIME OF PERIOD	END H(1)	ENERGY BALANCE - CAL/CM2-MIN	RADIATION		CAL/CM2-MIN DAT(7)		
			LE(1)	H(2)	QS(5)	QS(6)	
5	0.000	0.059	0.004	-C.063	0.000	0.000	C.609
6	-C.056	0.106	0.026	-C.056	0.020	0.020	0.726
7	0.000	-0.015	0.033	0.012	0.073	0.033	0.820
8	-0.056	-0.206	-0.032	C.264	0.153	0.035	0.980
9	-0.224	-0.016	-0.006	C.246	0.380	0.078	1.143
10	-0.224	-0.284	-C.016	C.524	0.873	0.161	1.518
11	-0.613	-0.347	-0.031	0.591	1.095	0.157	1.703
12	-0.558	-0.267	-C.031	C.356	1.217	0.137	1.885
13	-0.837	0.006	-C.028	C.859	1.155	0.135	1.826
14	-0.837	-0.004	-C.025	C.356	1.113	0.133	1.816
15	-0.446	0.210	-C.017	C.253	0.403	0.075	0.961
16	0.030	-0.057	-C.028	C.925	0.253	0.053	0.640
17	-0.168	-0.030	-C.011	0.239	0.393	0.075	0.954
18	-0.056	-0.037	-C.017	C.100	0.256	0.052	0.861
19	-0.168	0.153	-0.002	C.017	0.135	0.035	0.730
20	-0.112	0.190	-C.001	-C.077	0.035	0.015	0.621
21	0.000	0.078	C.001	-C.079	0.000	0.000	0.587
22	0.000	0.296	C.201	-C.297	0.000	0.000	0.570

(1) LE FROM LYSIMETER, (-) SIGN INDICATES FLUX AWAY FROM SURFACE

(2) SENSIBLE HEAT FLUX, H=-(LE+G+RN), (3) G = SOIL HEAT FLUX

(4) RN = NEI RADIATION, (5) QS = INCIDING GLOBAL SOLAR RADIATION

(6) QS = REFLECTED GLOBAL SOLAR, (7) QS = INCIDING ALL WAVE RADIATION

AVERAGE HOURLY LYSIMETER EVAPORATION, RADIATION, AND SOIL HEAT FLUX RATES

LYSIMETER SITE Y102-C CG SHOCKTON OHIO

DATE - 8/ 27/ 69

TIME OF PERIOD	END LE(1)	ENERGY BALANCE - CAL/CM2-MIN			RADIATION COMPONENTS - CAL/CM2-MIN		
		H(2)	G(3)	RN(4)	QS(5)	QS(6)	QAT(7)
6	0.000	0.059	0.015	-0.074	0.000	0.000	0.419
7	0.000	0.029	0.014	-0.043	0.090	0.038	0.506
8	-0.112	-0.026	0.008	0.130	0.341	0.096	0.744
9	-0.280	-0.076	0.001	0.355	0.643	0.145	1.071
10	-0.280	-0.294	-0.014	0.588	0.887	0.176	1.336
11	-0.502	-0.179	-0.015	0.700	1.085	0.176	1.538
12	-0.502	-0.278	-0.027	0.807	1.195	0.203	1.664
13	-0.558	-0.253	-0.035	0.846	1.213	0.203	1.708
14	-0.670	-0.104	-0.019	0.793	1.142	0.187	1.647
15	-0.614	-0.146	-0.014	0.774	1.018	0.170	1.530
16	-0.280	-0.303	-0.010	0.593	0.837	0.143	1.328
17	-0.280	-0.105	-0.007	0.392	0.578	0.100	1.062
18	-0.168	0.004	-0.004	0.168	0.273	0.053	0.782
19	-0.168	0.194	0.003	-0.029	0.006	0.003	0.520
20	-0.056	0.113	0.007	-0.064	0.000	0.000	0.460
21	-0.056	0.120	0.008	-0.072	0.000	0.000	0.467
22	-0.056	0.106	0.006	-0.056	0.000	0.000	0.471
23	0.000	0.060	0.008	-0.068	0.000	0.000	0.475

(+) LE FROM LYSIMETER, (-) SIGN INDICATES FLUX AWAY FROM SURFACE

(2) SENSIBLE HEAT FLUX,  $H = (LE + G + RN)$ , (3)  $G = \text{SOIL HEAT FLUX}$

(4)  $RN = \text{NET RADIATION}$ , (5)  $QS = \text{INCIDING GLOBAL SOLAR RADIATION}$

(6)  $RS = \text{REFLECTED GLOBAL SOLAR}$ , (7)  $QAT = \text{INCIDING ALL WAVE RADIATION}$

AVERAGE HOURLY LYSIMETER EVAPORATION, RADIATION, AND SOIL HEAT FLUX RATES

LYSIMETER SITE Y102-C, CESSNECION OHIO

DATE - 10/14/69

TIME END OF PERIOD	ENERGY BALANCE - LE(1)	CAL / CM2-MIN	RADIATION COMPONENTS - CAL / CM2-MIN
	H(2)	RN(3)	QS(5) RQS(6) QAT(7)
6	-0.056	0.093	C.00C -0.037 0.000 0.300 0.489
7	-0.112	0.149	C.00C -0.037 0.000 0.000 0.478
8	-0.112	0.132	0.00C -0.02C 0.063 0.005 0.526
9	-0.084	-0.020	0.00C 0.104 0.188 0.033 0.637
10	-0.056	-0.079	0.00C 0.135 0.258 0.045 0.703
11	-0.146	-0.024	C.00C 0.164 0.247 0.045 0.683
12	-0.123	-0.034	C.00C 0.157 0.306 0.050 0.748
13	-0.185	-0.136	C.00C 0.321 0.463 0.075 0.890
14	-0.112	-0.123	C.00C 0.235 0.412 0.067 0.849
15	-0.096	-0.074	0.00C 0.164 0.286 0.048 0.707
16	-0.056	-0.049	0.00C 0.105 0.353 0.061 0.723
17	-0.056	0.013	0.00C 0.043 0.203 0.043 0.548
18	-0.056	0.208	C.00C -C.152 0.043 0.004 0.370
19	-0.056	0.214	0.00C -C.158 0.000 0.000 0.348
20	-0.056	0.215	0.00C -C.159 0.000 0.000 0.346

(1) LE FROM LYSIMETER, (-) SIGN INDICATES FLUX AWAY FROM SURFACE

(2) SENSIBLE HEAT FLUX,  $\dot{F} = -(LE + G + RN)$ , (3) G = SOILHEAT FLUX

(4) RN = NET RADIATION, (5) QS = INCOMING GLOBAL SOLAR RADIATION

(6) RQS = REFLECTED GLOBAL SOLAR, (7) QAT = INCOMING ALL WAVE RADIATION

AVERAGE HOURLY LYSIMETER EVAPORATION, RADIATION, AND SOIL HEAT FLUX RATES

LYSIMETER SITE Y102-C, CESSHOCK, OHIO

DATE - 10/16/69

TIME OF PERIOD	ENERGY BALANCE	CAL/CM2-MIN	RADIATION COMPONENTS - CAL/CM2-MIN
	H(1)	H(2)	QS(5)
	LE(1)	LE(3)	ROS(6)
8	-0.101	0.097	0.004
9	-0.067	0.035	0.032
10	-0.056	-0.121	0.177
11	-0.101	-0.199	0.300
12	-0.190	-0.165	0.355
13	-0.146	0.011	0.135
14	-0.134	-0.013	0.147
15	-0.123	0.011	0.112
16	-0.168	0.149	0.019
17	-0.112	0.130	-0.018
18	-0.056	0.107	-0.051
19	-0.056	0.116	-0.060

(1) LE FROM LYSIMETER. (+) SIGN INDICATES FLUX AWAY FROM SURFACE

(2) SENSIBLE HEAT FLUX, H = (LE+G+RN), (3) LE = SOIL HEAT FLUX

(4) RN = NET RADIATION, (5) QS = INCOMING GLOBAL SOLAR RADIATION

(6) ROS = REFLECTED GLOBAL SOLAR, (7) QAI = INCOMING ALL WAVE RADIATION

- SMOOTHED PROFILE DATA FROM LOG-LINEAR PLOTS OF TEMPERATURE, HUMIDITY, AND WIND

LYSIMETER SITE Y102-C

DATE - 5/ 21 69

TIME END OF PERIOD	TEMPERATURE (C) 10	100	ABS. HUMIDITY 1C	100	WIND (CM/SEC) 100
5	8.05	1C.00	5.17	5.10	58.
6	8.10	5.86	5.20	5.25	68.
7	9.58	5.49	5.42	5.30	77.
8	12.73	11.16	5.90	5.65	87.
9	17.36	14.53	6.92	6.08	122.
10	22.03	18.33	7.67	6.46	155.
11	24.86	20.97	7.78	6.86	165.
12	25.82	22.47	7.86	6.94	196.
13	27.67	23.95	8.32	7.35	256.
14	28.48	24.71	8.49	7.50	251.
15	28.55	25.34	9.02	7.97	230.
16	28.06	25.23	9.40	8.64	250.
17	26.75	24.58	9.23	8.50	265.
18	24.62	24.05	8.44	8.64	232.
19	21.85	22.42	8.33	8.41	183.
20	18.70	20.30	8.03	8.13	112.
21	16.52	18.94	7.24	7.39	97.
22	15.42	17.74	7.14	7.31	117.
					175.

HEIGHT OF MEASUREMENTS = 1C AND 100 CM.

Z0 = 0.10 CM D = 0.0 CM CROP HEIGHT = 0. CM

SMOOTHED PROFILE DATA FROM LOG-LINEAR PLOTS OF TEMPERATURE, HUMIDITY, AND WIND

## LYSIMETER SITE Y102-C COSHOCOTON OHIO

DATE - 5/ 22/ 69

TIME END OF PERIOD	TEMPERATURE (C)	ABS. HUMIDITY (GM/M3)			WIND (CM/SEC) 100
		100	10	100	
5	8.06	8.89	7.54	7.38	70.
6	8.05	8.89	7.40	7.46	64.
7	9.37	9.54	8.05	7.93	62.
8	11.82	10.97	9.43	8.50	46.
9	12.82	12.49	10.00	9.06	28.
10	12.50	11.97	10.05	9.15	56.
11	11.17	11.37	9.53	9.35	150.
12	11.34	11.39	9.89	9.62	127.
13	12.59	12.18	10.52	9.98	101.
14	13.98	13.60	11.21	9.90	202.
15	15.43	14.80	12.02	9.92	116.
16	15.92	15.63	12.16	9.87	193.
17	14.91	15.25	11.36	10.05	106.
18	14.05	14.46	11.14	10.17	213.
19	12.68	13.08	10.29	9.75	218.
20	11.66	11.52	9.64	8.66	109.
21	10.83	10.84	8.94	8.05	257.
22	10.44	10.92	8.76	7.88	101.
					202.
					243.
					109.

HEIGHT OF MEASUREMENTS = 10 AND 100 CM.

Z0 = 0.10 CM D = 0.0 CM CROP HEIGHT = 0. CM

## SMOOTHED PROFILE DATA FROM LOG-LINEAR PLOTS OF TEMPERATURE, HUMIDITY, AND WIND

LYSIMETER SITE Y102-C COSHOUTON OHIO

DATE - 6/ 26/ 69

TIME END OF PERIOD	TEMPERATURE (C) 150	250	ABS. HUMIDITY (GM/M3) 15C	250	WIND (CM/SEC)	
					150	250
5	21.37	21.51	17.90	17.85	133.	160.
6	21.03	21.15	17.59	17.54	133.	160.
7	21.47	21.45	17.70	17.47	165.	200.
8	23.72	23.55	19.12	18.81	165.	200.
9	25.32	25.15	19.85	19.47	179.	217.
10	27.06	26.99	21.14	20.27	179.	217.
11	28.47	28.40	21.55	20.60	235.	285.
12	29.90	29.82	21.80	20.85	293.	352.
13	29.55	29.52	21.04	20.07	320.	385.
14	30.63	30.69	20.60	19.70	360.	438.
15	30.97	31.01	19.87	19.03	360.	438.
16	31.52	31.57	19.66	19.00	310.	370.
17	31.16	31.20	19.90	19.25	310.	370.
18	30.20	30.25	20.19	19.90	255.	307.
19	28.90	28.96	19.37	19.15	179.	217.
20	27.75	27.80	19.50	19.32	187.	225.
21	27.15	27.33	19.31	19.20	172.	207.
22	26.36	26.64	16.31	19.12	153.	183.

HEIGHT OF MEASUREMENTS = 15C AND 25C CM.

Z0 = 2.00 CM      n = 50.0 CM      CROP HEIGHT = 75. CM

SMOOTHED PROFILE DATA FROM LOG-LINEAR PLOTS OF TEMPERATURE, HUMIDITY, AND WIND

LYSIMETER SITE Y102-C CCSHOCTON OHIO

DATE - 7/ 24/ 69

TIME END OF PERIOD	TEMPERATURE (C)	350	250	350	250	350	WIND (CM/SEC)
5	19.57	15.76	16.62	16.80	32.	44.	
6	18.88	18.93	16.04	16.19	51.	67.	
7	19.30	19.25	16.57	16.52	40.	55.	
8	19.61	19.53	16.96	16.80	41.	56.	
9	20.32	20.15	17.48	17.26	41.	56.	
10	23.15	22.76	18.11	17.85	36.	48.	
11	24.59	24.12	16.90	16.32	62.	81.	
12	26.07	25.73	17.26	16.66	86.	116.	
13	26.97	26.67	17.15	16.42	109.	144.	
14	27.15	26.85	17.73	17.15	186.	236.	
15	26.22	26.15	16.46	16.00	115.	155.	
16	24.40	24.50	17.25	16.72	86.	116.	
17	24.50	24.25	18.08	17.74	102.	132.	
18	24.28	24.08	16.97	16.80	83.	111.	
19	23.48	23.45	17.35	17.12	70.	95.	
20	23.11	23.20	17.98	17.80	17.	22.	
21	22.45	22.52	17.42	17.20	82.	107.	
22	22.00	22.09	17.17	17.00	41.	56.	

HEIGHT OF MEASUREMENTS = 250 AND 350 CM.

Z0 = 15.00 CM D = 150.0 CM CROP HEIGHT = 240. CM

## SMOOTHED PROFILE DATA FROM LOG-LINEAR PLOTS OF TEMPERATURE, HUMIDITY, AND WIND

LYSIMETER SITE Y102-C COSHOC TION OHIO

DATE - 8/ 27/ 69

TIME END OF PERIOD	TEMPERATURE (C) 250	350	ABS. HUMIDITY (GM/M3) 25C	350	WIND (CM/SEC) 250	350
6	11.93	12.65	9.02	9.06	90.	125.
7	12.60	12.80	9.48	9.45	100.	143.
8	13.95	13.60	9.17	9.02	105.	152.
9	16.70	16.30	10.12	9.97	73.	104.
10	18.80	18.60	10.45	10.30	80.	112.
11	20.85	20.61	10.7C	10.42	64.	89.
12	22.45	21.90	11.05	10.61	93.	133.
13	23.48	23.14	11.35	10.95	82.	115.
14	24.07	23.86	11.01	10.67	82.	115.
15	24.63	24.37	10.72	10.48	56.	82.
16	24.75	24.34	10.37	10.14	74.	107.
17	25.26	24.96	10.71	10.43	46.	67.
18	24.40	24.43	10.13	10.00	26.	37.
19	22.22	22.45	9.97	9.85	39.	54.
20	21.76	21.96	9.83	9.76	43.	61.
21	21.70	21.77	9.83	9.76	43.	61.
22	19.75	19.74	9.82	9.60	22.	32.
23	18.90	18.90	10.37	10.23	31.	44.

HEIGHT OF MEASUREMENTS = 25C AND 35C CM.

Z0 = 20.00 CM D = 150.0 CM CROS HEIGHT = 240. CM.

SMOOTHED PROFILE DATA FROM LOG-LINEAR PLOTS OF TEMPERATURE, HUMIDITY, AND WIND

LYSIMETER SITE Y102-C COSHOCOTON OHIO

DATE - 10/ 14/ 65

TIME END OF PERIOD	TEMPERATURE (C)	ABS. HUMIDITY (GM/M3)	WIND (CM/SEC)
	150	250	150
6	9.18	5.19	7.06
7	8.90	8.85	6.91
8	8.45	8.40	6.50
9	8.74	8.66	5.92
10	8.95	8.60	5.48
11	9.34	9.17	5.32
12	9.76	9.58	5.48
13	10.87	10.52	5.85
14	10.78	10.52	5.66
15	10.60	10.38	5.62
16	10.25	10.13	5.40
17	9.80	9.99	5.32
18	8.50	8.68	5.15
19	7.10	7.28	5.11
20	3.80	3.96	4.01
			3.99
			130.
			167.

HEIGHT OF MEASUREMENTS = 150 AND 250 CM.

Z0 = 8.00 CM D = 50.0 CM CROP HEIGHT = 130. CM

SMOOTHED PROFILE DATA FROM LOG-LINEAR PLOTS OF TEMPERATURE, HUMIDITY, AND WIND

LYSIMETER SITE Y102-C CESSNACTION OHIO

DATE - 10/ 16/ 69

TIME END OF PERIOD	TEMPERATURE (C) 10 100	ABS. HUMIDITY 1C 100	WIND (CM/SEC) 10 100
8	11.47	11.51	9.04
9	12.29	12.25	9.36
10	13.84	13.65	8.97
11	15.72	14.99	8.95
12	16.41	15.35	8.22
13	15.37	14.86	8.51
14	14.77	14.48	8.13
15	14.62	14.31	7.84
16	13.54	13.63	7.42
17	12.35	12.59	7.03
18	11.58	12.02	7.19
19	10.97	11.45	7.18
			7.02
			95.
			229.

HEIGHT OF MEASUREMENTS = 1C AND 100 CM.

Z0 = 0.10 CM D = 0.0 CM CROP HEIGHT = 0. CM

SMOOTHED PROFILE DATA FROM LOG-LINEAR PLOTS OF TEMPERATURE, HUMIDITY, AND WIND  
 WATERSHED SAMPLING SITE - CONSTRUCTION OHIO

DATE - 7/ 24/ 69

TIME END OF PERIOD	TEMPERATURE (C)	ABS. HUMIDITY (GM/M3)	WIND (CM/SEC)
	250	350	250
5	18.55	18.67	15.70
6	18.36	18.30	15.70
7	18.75	18.68	16.05
8	19.02	18.92	16.31
9	19.90	19.84	16.84
10	22.75	22.08	16.80
11	24.18	23.55	15.81
12	25.49	24.75	16.52
13	26.10	25.62	16.92
14	26.10	25.58	16.62
15	25.17	24.94	15.72
16	23.45	23.13	16.65
17	23.40	23.00	17.13
18	23.10	22.72	16.22
19	22.75	22.42	17.13
20	21.60	21.52	17.30
21	21.26	21.26	16.72
22	20.86	20.75	16.42

HEIGHT OF MEASUREMENTS = 250 AND 350 CM.

Z0 = 15.00 CM      0 = 150.0 CM      CROP HEIGHT = 240. CM

SMOOTHED PROFILE DATA FROM LOG-LINEAR PLOTS OF TEMPERATURE, HUMIDITY, AND WIND

WATERSHED SAMPLING SITE COSHOCOTON OHIO

DATE - 8/ 27/ 69

TIME END OF PERIOD	TEMPERATURE (C)	ABS. HUMIDITY (GM/M3)	WIND (CM/SEC)
250	350	250	350
6	10.77	11.15	8.22
7	10.18	10.23	8.64
8	12.94	12.75	8.72
9	15.48	15.26	9.43
10	18.03	17.62	9.78
11	19.22	18.70	9.37
12	20.70	26.20	10.00
13	21.67	21.38	10.10
14	22.33	21.97	9.95
15	23.20	22.80	9.74
16	23.42	23.03	9.54
17	23.62	23.35	10.12
18	21.97	21.92	9.72
19	18.14	18.47	7.65
20	16.67	17.00	6.80
21	16.23	16.46	6.35
22	15.67	15.82	7.34
23	14.76	14.73	7.62

HEIGHT OF MEASUREMENTS = 250 AND 350 CM.

Z0 = 20.00 CM D = 150.0 CM CROP HEIGHT = 240. CM

## SMOOTHED PROFILE DATA FROM LOG-LINEAR PLOTS OF TEMPERATURE, HUMIDITY, AND WIND

## WATERSHED SAMPLING SITE - CONSTRUCTION OHIO

DATE - 10/ 14/ 65

TIME END OF PERIOD	TEMPERATURE (C)	ABS. HUMIDITY (GM/M3)	WIND (CM/SEC)
150	250	150	150
10	9.11	8.99	150
6	8.81	8.85	189.
7	8.38	8.42	189.
8	8.25	8.29	189.
9	8.75	8.65	176.
10	9.45	9.33	220.
11	10.03	9.82	221.
12	11.04	10.62	230.
13	10.75	10.45	173.
14	10.94	10.75	183.
15	10.67	10.52	165.
16	9.80	9.84	160.
17	7.75	7.99	167.
18	6.43	6.71	150.
19	5.98	6.24	135.
20	5.27	5.12	137.

HEIGHT OF MEASUREMENTS = 150 AND 250 CM.

Z0 = 8.00 CM D = 50.0 CM CROP HEIGHT = 130. CM

## SMOOTHED PROFILE DATA FROM LOG-LINEAR PLOTS OF TEMPERATURE, HUMIDITY, AND WIND

## WATERSHED SAMPLING SITE CASHCATION OHIO

DATE - 10/16/ 69

TIME END OF PERIOD	TEMPERATURE (C)	ABS. HUMIDITY (GM/M3)			WIND (CM/SEC)
		100	10	100	
8	11.15	11.30	8.99	8.89	176.
9	11.72	11.95	9.26	9.18	352.
10	12.94	13.12	8.81	8.73	420.
11	14.19	14.14	7.98	7.86	553.
12	15.08	14.87	7.72	7.70	544.
13	13.97	13.80	7.62	7.58	592.
14	14.11	13.87	7.72	7.67	585.
15	13.92	13.60	7.37	7.33	520.
16	12.78	12.88	6.81	6.90	532.
17	11.94	12.34	6.74	6.82	532.
18	11.20	11.71	6.85	6.93	447.
19	10.71	11.17	6.87	6.92	386.
					296.

HEIGHT OF MEASUREMENTS = 10 AND 100 CM.

Z0 = 0.10 CM D = 0.0 CM CROP HEIGHT = 0. CM

## APPENDIX D—AVERAGE HOURLY EVAPORATION

This appendix reports average hourly evapotranspiration by the various meteorological equations using the smoothed profile data and average hourly radiation data. Also presented are the computed Bowen Ratio (B) and Richardson's Number (R<sub>I</sub>).

The values in the probable error columns gave the range of probable error that can be expected in each computed value on the basis of instrument accuracy and sensitivity. Missing data are due to equipment malfunction, as indicated by an asterisk.

COMPUTED ET BY VARIOUS METEOROLOGICAL EQUATIONS = COSHACON 1969 - LYSIMETER SITE

5/ 2/69 CROP HEIGHT = 0, D = 0.0 ZO = 0.1 ALL IN CM.

GRAM CALORIES/CM2-MIN FOR PERIOD ENDING:

HR LYS BOWEN AERO AER-C-K AERO-D PCLEN PROBABLE ERROR ANALYSIS  
ET ET ET ET ET ET AERO AERO PET

5	-C.000	0.005	0.001	0.000	-0.054	-27.89	0.725	0.001	0.000	0.000	0.017
6	-0.000	-0.011	-C.CC3	-0.003	-0.001	-0.050	10.51	0.425	0.003	0.001	0.001
7	-0.000	-0.069	0.005	0.006	0.007	-0.028	0.36	-0.018	0.023	0.001	0.018
8	0.056	0.018	0.C13	0.C31	C.049	0.071	2.72	-0.263	0.008	0.002	0.005
9	0.112	0.091	0.C57	C.131	0.204	0.202	1.46	-0.224	0.013	0.006	0.014
10	0.223	C.154	0.101	0.218	0.337	0.344	1.35	-0.198	0.013	0.009	0.019
11	0.167	C.180	0.C82	0.174	C.268	C.477	1.80	-0.186	0.011	0.007	0.014
12	0.167	0.227	0.C56	0.17C	0.252	0.564	1.56	-0.113	0.012	0.007	0.011
13	0.167	0.238	0.135	0.208	0.294	0.655	1.62	-0.071	0.012	0.007	0.011
14	0.223	0.221	0.138	0.213	C.301	0.624	1.61	-0.072	0.012	0.007	0.019
15	0.112	0.222	0.131	0.204	C.290	0.556	1.30	-0.075	C.014	0.007	0.011
16	0.112	0.15C	0.107	0.153	C.210	0.465	1.55	-0.055	0.012	0.006	0.008
17	0.056	C.096	0.105	C.139	C.134	0.337	1.27	-C.039	0.014	0.005	0.007
18	-0.000	-C.063	-0.021	-0.024	-0.028	C.166	-1.45	-0.013	0.069	0.001	0.001
19	-0.000	-0.026	-0.005	-0.007	-0.006	0.031	2.79	0.022	0.008	0.001	0.027
20	-0.000	-0.024	-0.008	-0.005	-0.003	-0.049	5.28	0.159	C.005	0.001	0.001
21	-0.000	-0.023	-0.021	-0.011	-0.003	-0.056	5.49	0.332	0.005	0.001	0.002
22	-0.000	-0.025	-0.014	-0.014	-0.004	-C.048	4.89	0.210	0.005	0.002	0.002

BOWEN = ET BY BOWEN RATIO METHOD

AEROD = ET BY AERODYNAMIC -DAVIS STABILITY CORRECTION

AER-C-K = ET BY AERODYNAMIC -KEYPS STABILITY CORRECTION

LYS = OBSERVED ET FROM LYSIMETER

PCLEN = POTENTIAL ET BY COMBINATION EQUATION

COMPUTED ET BY VARIOUS METEOROLOGICAL EQUATIONS = CONVENTION 1962 - LYSIMETER SITE

5/22/69		CROP HEIGHT = 0.		D = 0.0		Z = 0.1		ALL IN CM.	
		GRAM CALORIES/CM2-MIN FOR PERIOD ENDING:				± GRAM CALORIES/CM2 - MIN			
HR.	LYS	BOWEN	AERO	AEROK	AERO-D.	PCTEN	ET	ET	ET
5	0.004	0.066	0.013	0.008	-0.061	-2.97	0.034	0.016	0.001
6	0.020	-0.022	-0.026	-0.006	-0.003	-0.063	5.05	0.057	0.001
7	0.047	*	0.011	0.008	-0.033	-0.54	0.013	0.072	0.001
8	0.075	C.027	0.048	0.086	0.128	0.027	0.43	-0.119	0.022
9	0.100	-0.011	0.028	0.052	0.079	-0.005	0.17	-0.130	0.027
10	0.105	-0.021	0.072	0.091	0.116	-0.009	0.28	-0.030	0.024
11	RAIN	*	C.011	C.010	0.009	-0.034	-0.56	0.016	0.006
12	0.050	-0.049	0.029	0.029	C.029	-0.022	-0.09	0.002	0.002
13	0.083	0.096	0.063	0.071	0.080	0.083	0.36	-0.011	0.023
14	0.225	0.314	0.192	0.206	0.223	0.227	0.14	-0.006	0.027
15	0.345	C.407	0.269	0.304	C.353	0.302	0.14	-0.013	0.027
16	0.195	0.316	0.225	0.249	C.232	0.223	0.06	-0.010	0.029
17	0.140	C.241	0.147	0.139	C.124	C.143	-0.13	C.009	0.036
18	0.130	-0.003	0.110	0.101	0.091	0.008	-0.21	0.011	0.039
19	0.042	*	0.076	0.073	0.067	-0.046	-0.37	0.007	0.050
20	0.018	*	0.105	0.111	0.118	-0.053	0.07	-0.004	0.029
21	0.013	*	0.126	0.128	0.128	-0.055	-0.01	0.000	0.031
22	-0.006	*	0.115	0.110	0.102	-0.049	-0.23	0.007	0.041
									0.005
									0.019

BOWEN = ET BY BOWEN RATIO METHOD

AEROK = ET BY AERODYNAMIC - CAVIS STABILITY CORRECTION

AEROD = ET BY AERODYNAMIC - KEYS STABILITY CORRECTION

LYS = OBSERVED ET FROM LYSIMETER

PCTEN = POTENTIAL ET BY COMBINATION EQUATION

\*See Footnote at end of Tables

COMPUTED ET BY VARIOUS METEOROLOGICAL EQUATIONS - CASHOCION 1969 - LYSIMETER SITE

8/26/69 - CROP HEIGHT = 75.0 - D = 50.0 - Z = 2.0 - ALL IN CM.

GRAM CALORIES/CM<sup>2</sup>-MIN FOR PERIOD ENDING:

HR	LYS	BOWEN	AERO	AERCK	AERO-D	PETEN	ET	ET	ET	PROBABLE ERROR ANALYSIS		
										6	RI	BOWEN
5	-0.000	*	0.013	0.013	0.006	-0.071	-1.59	0.064	0.058	0.004	0.004	0.024
6	-0.000	*	0.013	0.014	0.007	-0.025	-1.33	0.055	0.149	0.004	0.004	0.023
7	0.112	0.080	0.094	0.100	0.077	0.04	-0.005	0.030	0.024	0.025	0.025	0.025
8	0.278	0.209	0.130	0.178	0.239	0.223	0.25	-0.046	0.025	0.033	0.045	0.026
9	0.278	0.287	0.171	0.226	0.298	0.310	0.20	-0.039	0.027	0.042	0.055	0.028
10	0.558	0.516	0.381	0.439	0.518	0.470	0.04	-0.016	0.031	0.094	0.107	0.030
11	0.725	0.717	0.545	0.598	0.669	0.681	0.03	-0.009	0.031	0.121	0.130	0.039
12	0.837	0.851	0.643	0.696	0.756	0.862	0.04	-0.007	0.031	0.135	0.144	0.051
13	0.892	0.809	0.721	0.748	0.774	0.835	0.01	-0.002	0.032	0.148	0.151	0.057
14	0.837	0.873	0.757	0.787	0.753	0.934	-0.03	0.003	0.034	0.158	0.153	0.073
15	0.837	0.791	0.745	0.743	0.720	0.909	-0.02	0.002	0.033	0.148	0.145	0.080
16	0.613	0.715	0.449	0.438	0.413	0.821	-0.03	0.004	0.034	0.094	0.090	0.073
17	0.502	0.488	0.442	0.435	0.414	0.634	-0.03	0.004	0.033	0.093	0.090	0.070
18	0.278	0.247	0.171	0.164	0.152	0.367	-0.08	0.006	0.035	0.037	0.035	0.054
19	0.112	0.054	0.094	0.083	0.074	0.160	-0.13	0.013	0.036	0.023	0.020	0.040
20	0.112	*	0.077	0.076	0.063	0.042	-0.13	0.011	0.036	0.019	0.017	0.037
21	0.056	*	0.040	0.015	0.022	-0.013	-0.85	0.048	0.640	0.010	0.004	0.034
22	-0.000	*	0.059	0.060	0.024	0.014	-0.76	0.102	0.148	0.017	0.017	0.030

BOWEN = ET BY BOWEN RATIO METHOD

AERCO = ET BY AERODYNAMIC - CAVIS STABILITY CORRECTION

AERCK = ET BY AERODYNAMIC - KEYS STABILITY CORRECTION

LYS = OBSERVED ET FROM LYSIMETER

PETEN = POTENTIAL ET BY COMBINATION EQUATION

\*See Footnote at end of Tables.

- COMPUTED ET BY VARIOUS METEOROLOGICAL EQUATIONS = COSHOCION 1959. - LYSIMETER SITE

- - - - - 7/24/65 - - - C'DP HEIGHT = 240. - D = 150.0 - - - 20 = 15.0. - - - ALL IN CM. - - - - -

- - - - - GRAM CALORIES/CM2-MIN FOR PERIOD ENDING - - - - - ± GRAM CALORIES/CM2 - MIN

HR.	LYS ET	BOWEN FT	AERO FT	AERO-K ET	PROTEN ET	B RI	R1	BOWEN AERO	PROBABLE ERROR ANALYSIS PET
5	-0.000	-0.041	-0.027	-0.027	-0.006	-0.038	-0.47	0.442	0.021
6	0.056	-0.044	-0.028	-0.029	-0.014	-0.031	0.16	0.066	0.027
7	-0.009	0.011	0.055	0.014	0.020	0.011	0.45	-0.075	0.021
8	0.056	0.051	0.029	0.052	0.077	0.042	0.23	-0.119	0.025
9	0.224	0.181	0.044	0.096	0.150	0.169	0.35	-0.253	0.024
10	0.224	0.314	0.165	0.270	0.398	0.65	-0.897	0.020	0.030
11	0.613	0.493	0.132	0.398	0.638	0.588	0.36	-0.429	0.024
12	0.558	0.663	0.214	0.390	0.582	0.795	0.26	-0.124	0.026
13	0.837	0.712	0.300	0.476	0.682	0.879	0.19	-0.080	0.027
14	2.837	0.694	0.343	0.455	0.600	1.027	0.23	-0.039	0.027
15	0.446	0.224	0.213	0.243	0.243	0.437	0.07	-0.014	0.029
16	RAIN	0.064	0.181	0.107	0.109	0.170	-0.09	0.037	0.034
17	0.168	0.151	0.123	0.203	0.294	0.271	0.33	-0.092	0.024
18	0.056	0.062	0.055	0.094	0.136	0.195	0.52	-0.084	0.021
19	0.168	0.014	0.067	0.077	0.091	0.093	0.06	-0.016	0.029
20	0.112	*	0.010	0.010	0.001	-0.043	-0.24	1.191	0.042
21	-0.000	*	0.062	0.037	0.038	0.008	-0.15	0.037	0.037
22	-0.000	*	0.025	0.025	0.011	-0.038	-0.26	0.133	0.043

BOWEN = ET BY BOWEN RATIO METHOD

AERCD= ET BY AERODYNAMIC -DAVIS STABILITY CORRECTION

AERCK= ET BY AERODYNAMIC -KEYPS STABILITY CORRECTION

LYS= OBSERVED ET FROM LYSIMETER

PROTEN= POTENTIAL ET BY COMBINATION EQUATION

\*See Footnote at end of Tables.



COMPUTED EI BY VARIOUS METEOROLOGICAL EQUATIONS - COSHOCTON 1969 - LYSIMETER SITE

10/14/69		CROP HEIGHT = 130.		D = 50.0		Z = 8.0		ALL IN CM.			
GRAM CALORIES/CM <sup>2</sup> -MIN FOR PERIOD ENDING:											
HR	LYS	BOWEN		AERC-K		AERD		POLEN		PROBABLE ERROR ANALYSIS	
		ET	ET	ET	ET	ET	ET	B	RI	BOWEN	AERO
										AERO	PE
6	0.055	*	0.052	0.053	0.052	0.052	0.052	-0.06	0.001	0.034	0.011
7	0.112	*	0.024	0.026	0.028	0.028	0.028	0.60	-0.007	0.020	0.005
8	0.112	*	0.021	0.023	0.023	0.026	0.026	-0.60	-0.009	0.020	0.005
9	0.084	C.047	C.021	C.021	C.023	C.026	C.026	1.25	-0.009	0.016	0.004
10	0.056	0.068	0.052	0.052	0.055	0.069	0.331	1.32	-0.014	0.016	0.005
11	0.140	0.065	0.043	0.048	0.056	0.368	0.368	1.58	-0.012	0.011	0.012
12	0.123	C.053	0.022	0.028	0.036	0.283	0.283	2.04	-0.034	0.013	0.009
13	0.185	C.132	0.058	0.087	0.123	0.377	0.377	1.46	-0.069	0.014	0.005
14	0.112	0.063	0.020	0.029	0.041	0.324	0.324	2.82	-0.066	0.009	0.005
15	0.090	0.089	0.063	0.084	0.111	0.300	0.300	0.87	-0.041	0.017	0.015
16	0.056	0.038	0.017	0.021	C.025	0.284	0.284	1.83	-0.020	0.012	0.019
17	0.056	0.018	-0.005	-0.009	-0.004	0.237	0.237	1.40	0.059	0.013	0.005
18	0.056	*	0.022	0.012	0.013	0.063	0.063	-1.90	0.039	0.055	0.003
19	0.056	*	0.017	0.010	0.010	0.039	0.039	-2.43	0.039	0.005	0.003
20	0.056	*	0.008	0.004	0.004	0.040	0.040	-4.55	0.041	0.012	0.002
										0.001	0.050

BOWEN = ET BY BOWEN RATIO METHOD

AERD = EI BY AERODYNAMIC -CAVIS STABILITY CORRECTION

AERC-K = EI BY AERODYNAMIC -KEYS STABILITY CORRECTION

LYS = OBSERVED ET FROM LYSIMETER

POLEN = POTENTIAL ET BY COMBINATIONAL EQUATION

\*See Footnote at end of Tables.

COMPUTED ET BY VARIOUS METEOROLOGICAL EQUATIONS - COSHOCTON 1969 - LYSIMETER SITE

10/16/69 CROP HEIGHT = 0. D = 0.0 Z0 = 0.1 ALL IN CM.

GRAM CALORIES/CM2-MIN FOR PERIOD ENDING:

HR	LYS	BOWEN	AERO	AERD-K	AERD-D	POTEN	ET	RI	BOWEN	PROBABLE ERROR ANALYSIS	PE-T
	ET	ET	ET	ET	ET	ET	ET	ET	AERO	AERO	PE-T
8	0.101	0.004	0.071	0.072	0.071	0.020	-0.06	0.000	C.033	0.002	0.021
9	0.067	0.031	0.133	0.136	0.136	0.040	0.04	-0.300	0.030	0.003	0.023
10	0.056	0.159	0.203	0.208	0.211	0.167	0.13	-0.001	0.028	0.005	0.026
11	0.101	C.198	0.200	0.208	C.217	0.290	0.54	-0.003	C.020	0.004	0.005
12	0.190	0.167	0.111	0.115	0.128	0.355	1.16	-0.006	0.015	0.003	0.028
13	0.146	0.092	0.168	0.174	0.178	0.197	0.49	-0.002	0.021	0.003	0.031
14	0.134	0.104	0.058	C.1C1	0.102	0.195	0.44	-0.001	0.022	0.002	0.029
15	0.123	0.081	0.110	0.113	0.115	0.172	0.41	-0.001	0.022	0.002	0.028
16	0.168	C.023	0.087	0.088	C.088	0.106	-0.15	0.000	0.036	0.002	0.027
17	0.112	*	0.032	C.033	0.032	C.061	-0.87	0.001	0.258	0.001	0.024
18	0.056	0.191	0.032	0.031	0.030	0.018	-1.27	0.004	0.123	0.001	0.021
19	0.056	0.104	0.621	0.020	C.018	-0.002	-1.59	0.008	0.054	0.001	0.020

BOWEN - ET BY BOWEN RATTIC METHOD

AERD - ET BY AERODYNAMIC - DAVIS STABILITY CORRECTION

AERQK - ET BY AERODYNAMIC - KEYS STABILITY CORRECTION

LYS - OBSERVED ET FROM LYSIMETER

POTEN - POTENTIAL ET BY COMBINATION EQUATION

\*See Footnote at end of Tables.



COMPILED BY VARIOUS MEDICAL PHYSICAL EQUIPMENTS - CONSTRUCTION - 1969 - WATERSHED SITE

ALL IN CM.

GRAMMARESCHEN IN DER FERNSICHT

THE SOUTHERN

HR LYS BOWEN AERC AERC-K AERC-Q PG1EN PROBABLE ERROR ANALYSIS  
ET ET ET ET ET ET B RI BOWEN AERO AEROK PET

BOWEN - ET BY BOWEN RATIC MELTED

AERODYNAMIC STABILITY CORRECTION

STAVELIX CUPRERELIX 1980

卷之三

卷之三

COMPUTED ET BY VARIOUS METEOROLOGICAL EQUATIONS - COSHACIAN 1959 - WATERSHED SITE

10/16/69 CROP HEIGHT = 0. D = 0.3 ZD = 0.1 ALL IN CM.

GRAM CALORIES/CM<sup>2</sup>-MIN FOR PERIOD ENDING:

HR	GRAM CALORIES/CM <sup>2</sup> -MIN FOR PERIOD ENDING:						+ GRAM CALORIES/CM <sup>2</sup> - MIN				
	LYS	BOWEN	AEROD	AERCK	AERO-D	PCTEN	B	RI	BOWEN	PROBABLE ERROR ANALYSIS	
ET	ET	ET	ET	ET	ET	ET				AERO	AEROK
8	0.101	0.044	0.018	0.018	0.017	0.025	-0.77	0.002	0.137	0.001	0.001
9	0.067	*	0.016	0.016	0.016	0.047	-1.55	0.002	0.060	0.000	0.022
10	0.056	*	0.022	0.022	0.022	0.172	-1.18	0.001	0.851	0.001	0.026
11	0.101	0.252	0.035	0.035	0.035	0.287	0.20	-0.000	0.032	0.001	0.028
12	0.190	0.076	0.004	0.004	0.008	0.366	3.96	-0.001	0.009	0.000	0.031
13	0.146	0.049	0.014	0.014	0.014	0.202	1.95	-0.001	0.012	0.000	0.030
14	0.134	0.049	0.016	0.016	0.016	0.194	2.06	-0.001	0.011	0.000	0.028
15	0.123	0.027	0.014	0.014	0.014	0.181	3.22	-0.001	0.008	0.000	0.029
16	0.158	0.017	-0.026	-0.026	0.026	0.126	0.53	0.000	0.020	0.001	0.029
17	0.112	-0.003	-0.021	-0.021	-0.020	0.079	2.18	0.002	0.010	0.001	0.026
18	0.056	-0.010	-0.019	-0.019	-0.018	0.041	2.70	0.004	0.008	0.001	0.023
19	0.056	-0.010	-0.010	-0.009	-0.009	0.019	3.68	0.006	0.007	0.000	0.021

BOWEN - ET BY BOWEN RATIO METHOD

AEROD - ET BY AERODYNAMIC - DAVIS STABILITY CORRECTION

AERCK - FT BY AERODYNAMIC - KEVPS STABILITY CORRECTION

LYS - OBSERVED ET FROM LYSIMETER

PCTEN - POTENTIAL ET BY COMBINATION EQUATION

\*Some data were possibly in error because of equipment malfunction, thereby resulting in the computer data in the table also being in error. An asterisk designates the missing statistics. Results, however, may be recalculated by the method described in previous listings.

COMPOSED BY VARIOUS METEOROLOGICAL SITUATIONS - COSHACTON 1969 - WATERSHED SITE

1.10.1.4.16.9 CROP HEIGHT = 130. D = 50.0 Z0 = 3.0 ALL IN CM

GRAM CALORIES/CM2-MIN FCR PERIOD ENDING:

+ EGR M1000/1000 - NEW

PROBABLE ERROR ANALYSIS

6	C.056	*	0.068	0.063	0.057	C.056	-0.13	0.009	0.036	0.017	0.015	0.042
7	0.112	*	0.055	0.055	0.050	0.060	-0.15	0.009	0.037	0.014	0.013	0.043
8	0.112	*	0.053	0.049	0.044	0.086	-0.17	0.010	0.037	0.013	0.012	0.042
9	C.084	0.076	0.070	0.081	0.097	0.209	C.37	-0.017	0.023	0.016	0.018	0.063
10	C.056	0.120	0.101	0.117	C.139	C.270	0.34	-0.017	0.024	0.022	0.025	0.071
11	0.140	0.106	0.087	0.100	0.117	0.296	0.42	-0.015	0.023	0.019	0.021	0.080
12	0.123	0.115	0.096	0.121	0.121	0.273	0.72	-0.053	0.019	0.016	0.022	0.062
13	0.135	0.146	0.129	0.135	C.198	0.366	1.15	-0.100	0.015	0.020	0.033	0.069
14	0.112	0.163	C.056	0.148	0.214	0.319	0.65	-0.090	0.019	0.023	0.038	0.062
15	C.090	0.107	0.082	0.115	0.156	0.252	0.48	-0.051	0.021	0.021	0.029	0.060
16	C.056	0.091	0.064	0.086	0.114	0.244	0.48	-0.040	0.021	0.016	0.021	0.062
17	0.056	-0.051	0.073	0.065	C.058	C.113	-0.10	0.013	0.035	0.019	0.017	0.053
18	C.056	*	0.064	0.064	C.020	0.044	-1.03	0.082	1.048	0.012	0.012	0.044
19	0.056	*	C.041	0.041	C.018	0.030	-1.33	C.090	0.143	0.011	0.011	0.040
20	0.056	*	C.056	C.057	C.025	0.022	-0.89	0.084	0.771	0.015	0.015	0.038

BCKEN = ET AV BOWEN BATIC METHOD

卷之三

卷之三

卷之三

卷之三

\*See Footnote at end of Tables.